

Sensor and Simulation Notes

Note 223

March 1977

Revised

November 1977

CLEARED  
FOR PUBLIC RELEASE

PL/PA 5-12-97

Modes on a Finite-Width, Parallel-Plate Simulator  
II. Wide Plates

Lennart Marin  
Dikewood Corporation, Westwood Research Branch  
Los Angeles, California

Abstract

The higher-order TE and TM modes on two, parallel wide plates are investigated. By means of Laplace transforms and the Wiener-Hopf technique integral equations are obtained from which expressions for the transverse propagation constants and the field distributions of the modes are derived in the special case of wide plates. It is found that besides the TEM mode, the TE modes are the most important modes on the simulator. The propagation constants and the field distributions of the lowest TE modes depend mainly on the width of the plates and they are almost independent of the distance separating the plate provided that this distance is small compared to the plate's width.

Acknowledgement

Thanks go to Drs. K.S.H. Lee and K. Chen for many enlightening discussions. The interest shown by Drs. C.E. Baum, J.P. Castillo and Capt. L. Roberts is also much appreciated. We wish to thank Drs. S.W. Lee and R. Mittra for pointing out certain features of the results for the antisymmetric TE modes. A further investigation into this matter resulted in the issuance of this errata.

PL 96-1245

## Contents

	Page
Abstract	1
Section	
I	Introduction
II	Formulation of Integral Equations
III	Transverse Propagation Constants of Modes on Two Wide Plates
IV	Field Distribution of the Modes
References	44

## ILLUSTRATIONS

Figure		Page
1	Schematic picture of bounded-wave simulators.	5
2	Two, finite-width, parallel plates.	8
3	The path of integration $C$ in the inverse Laplace transform integral.	12
4	The paths of integration $C$ , $C_1$ , and $C_2$ in the complex $q'$ -plane.	23
5	The transverse propagation constants for the symmetric TM modes $(p'_{s,n})$ and the symmetric TE modes $(p''_{s,n})$ .	26
6	The roots of (70) and (71). Roots such that $ ph  \cdot < 1$ are the transverse propagation constants for the antisymmetric TM modes $(p'_{a,n})$ .	29
7	The transverse propagation constants for the antisymmetric TE modes $(p''_{a,n})$ .	33
8a	Transverse variation of the $E_y$ field component of the four lowest odd antisymmetric TE modes.	38
8b	Transverse variation of the $H_x$ field component of the four lowest odd antisymmetric TE modes.	39
8c	Transverse variation of the $H_z$ field component of the four lowest odd antisymmetric TE modes.	40
9a	Transverse variation of the $E_y$ field component of the four lowest even antisymmetric TE modes.	41
9b	Transverse variation of the $H_x$ field component of the four lowest even antisymmetric TE modes.	42
9c	Transverse variation of the $H_z$ field component of the four lowest even antisymmetric TE modes.	43

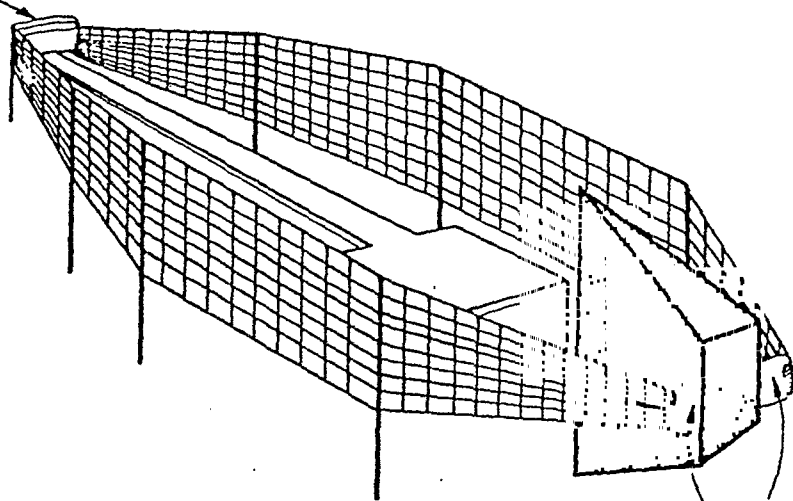
## SECTION I INTRODUCTION

Bounded-wave simulators all use two parallel, finite-width plates as the guiding structure for the simulated electromagnetic field, (see Fig. 1). The electromagnetic field on a parallel-plate simulator can be decomposed into a transverse electromagnetic (TEM) mode, higher-order transverse magnetic (TM) and transverse electric (TE) modes and a part due to the continuous spectrum. The properties of the TEM mode have been investigated exhaustively (refs. 1, 2, 3, 4, and 5), whereas the other parts of the field have been investigated only in some limiting cases. When the width of the plates is small compared to the distance between the plates it is found in ref. 6 that the TE modes are more attenuated as they propagate along the simulator than are the TM modes. The field lines and the field distributions of the two lowest TM modes are also investigated in ref. 6. To determine the relative importance of the TEM mode contribution to the total field, the time variation of the current induced on two parallel wires by two step-function slice generators is studied in ref. 7. It is found in this reference that the TEM mode constitutes the dominant part of the induced current provided one transit time between the wires has elapsed after the passage of the wavefront.

In this report we will consider two parallel plates where the width of each plate is much larger than the separating distance. In this case, the numerical solution of the integral equations derived in ref. 6 becomes very time consuming even on a fast computer. Therefore, based on Laplace-transform methods and the theory of Wiener and Hopf alternative integral equations are derived. Although both the integral equations derived in ref. 6 and those of this report are exact, those derived in the reference are most useful for numerical treatment when the distance separating the plates is comparable to or larger than their width, whereas those derived in this report are most useful when the distance separating the plates is comparable to or smaller than their width.

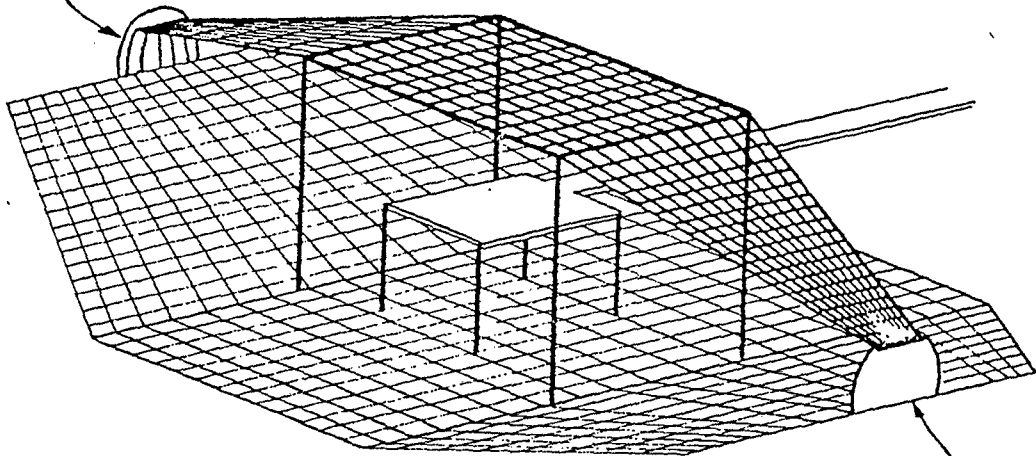
Integral equations for the transverse magnetic and transverse electric fields are derived in section II. The approach used in this report is based on Laplace transform techniques and follows the one in refs. 8 and 9 except that the Jones version of the Wiener-Hopf method (refs. 10 and 11) is invoked here. Although there exist different ways of deriving integral equations in the Laplace

TERMINATION



PULSERS

TERMINATION



PULSER

Figure 1. Schematic picture of bounded-wave simulators.

method used here seems to be the most expeditious one.

The integral equations derived in Section II are then used in Section III to obtain expressions for the transverse propagation constant in the special case where the width-to-separation ratio of the plates is large. It is found that in this case the TE modes have the smallest damping constant. This fact should be compared with the fact that the TM modes have the smallest damping constant when the plates are narrow. The field distributions of the lowest TE modes are calculated in Section IV. Except close to the edges of the simulator, the field distribution of the TE modes are almost uniform in the direction perpendicular to the plates and varies almost sinusoidally in the transverse direction parallel to the plates. It is also found that in a relatively large region around the center of the simulator all field components can be expressed in terms of an almost real function.

An approximate method of calculating the propagation constant on an open waveguide is given by Weinstein<sup>[14]</sup>. This method is based on the observation that when a waveguide mode on a semi-infinite parallel-plate waveguide, with near cut-off propagation constant reaches the open end of the waveguide it is reflected back with a reflection coefficient of absolute value close to unity. Weinstein's method is used in [24] to determine certain characteristics of the higher-order modes on an open parallel-plate waveguide. It is also used in [15,16] to find the resonance frequencies on open resonators, e.g., the Fabry-Perot resonator.

Numerous investigations have been devoted to the classical problem of scattering from an infinitely long strip or slit in a ground plane. Many of the techniques developed in solving this problem can in principle be used to treat the two-plate problem. One possible approach is the Fox integral-equation approach<sup>[17]</sup> where the problem of pulse diffraction by a slit is reduced to a set of Fredholm integral equations of the second kind which then are solved iteratively. Similar approaches have also been applied to the strip and slot problem by Millar<sup>[18,19]</sup> and Grinberg<sup>[20,21]</sup>. It should also be mentioned that the transverse propagation constants of the leaky modes on a strip were calculated in [22]. When solving this problem Fourier transform methods are used to derive an integral equation which is then solved using the Fredholm determinant theory.

## II. Formulation of Integral Equations

Consider an open waveguide formed by two infinitely long, perfectly conducting, parallel plates of finite width (Fig. 2). The width of each plate is denoted by  $2w$  and the distance separating the plates by  $2h$ . A coordinate system is introduced such that the  $z$ -axis coincides with the axis of the waveguide and the  $x$ - $y$  plane is the transverse plane of the waveguide with the  $x$ -axis parallel to the plates (see Fig. 2).

It is well known that the electromagnetic field on any uniform waveguide can be uniquely decomposed into two parts: one part with zero axial component of the magnetic field (TM-field, E-waves) and the other part with zero axial component of the electric field (TE-field, H-waves). Accordingly, in this section a derivation is first given of an integral equation for the transverse magnetic field and then a corresponding integral equation for the transverse electric field is derived.

### A. Transverse Magnetic Field

By taking the Laplace transform with respect to time (transform variable  $s$ ) and the spatial coordinate  $z$  (transform variable  $\zeta$ ) of the longitudinal component of the electric field one gets the following differential equation

$$\left[ \frac{\partial^2}{\partial x^2} + \frac{\partial^2}{\partial y^2} - p^2 \right] E_z = 0 \quad (1)$$

where  $E_z = E_z(x, y, \zeta, s)$  and  $p^2 = s^2 c^{-2} - \zeta^2$ , c.f. the notation used in [6]. To solve (1) one uses Laplace transform methods to get the integral representation of  $E_z$ ,

$$E_z(x, y, \zeta, s) = \frac{1}{2\pi i} \int_C \tilde{E}_z(q, y, \zeta, s) \exp(qx) dq \quad (2)$$

where the path of integration  $C$  is symmetric with respect to the origin in the complex  $q$ -plane. It will be discussed later how to choose  $C$  properly. It should be mentioned that the two-sided Laplace transform integral for  $E_z$  does not necessarily exist. Nevertheless, the representation (2) is still permissible provided that the path of integration  $C$  is properly chosen [23].

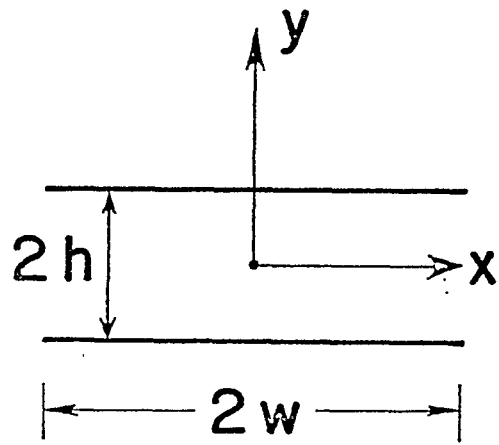
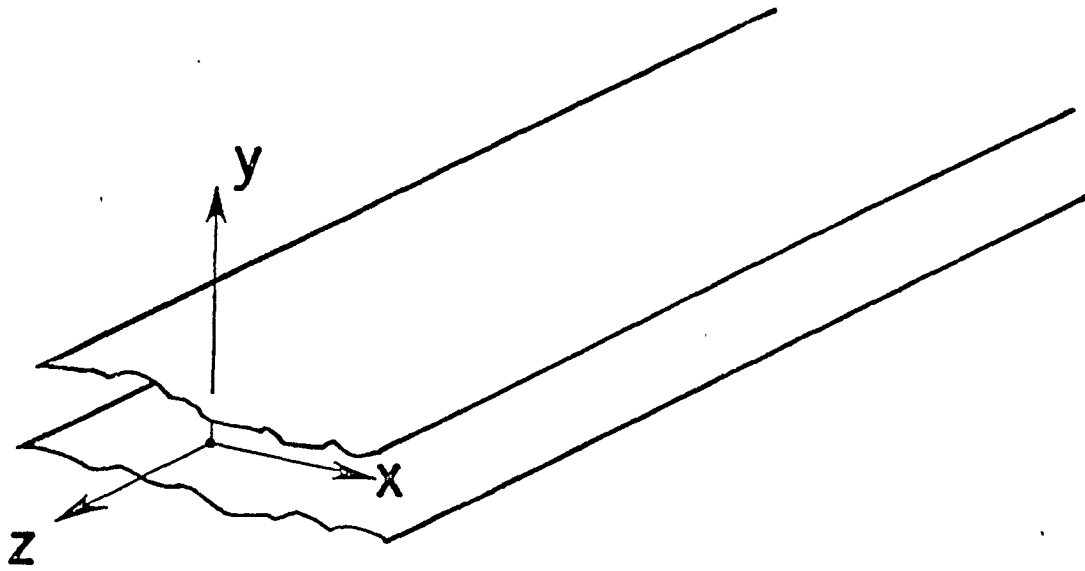


Figure 2. Two, finite-width, parallel plates.

Inserting (2) into (1) leads to the following differential equation for  $\tilde{E}_z$ ,

$$\left[ \frac{d^2}{dy^2} - p^2 + q^2 \right] \tilde{E}_z = 0. \quad (3)$$

Taking into account the outgoing wave condition for  $\tilde{E}_z$  at large values of  $|y|$  and that  $\tilde{E}_z$  is continuous for  $y = \pm h$  one obtains the following solution to (3),

$$\tilde{E}_z(q, y, \zeta, s) = \begin{cases} \tilde{E}_z(q, h, \zeta, s) \exp[-i\kappa(y - h)], & y > h \\ \tilde{E}_z(q, h, \zeta, s) \frac{\sin[\kappa(y+h)]}{\sin[2\kappa h]} - \tilde{E}_z(q, -h, \zeta, s) \frac{\sin[\kappa(y-h)]}{\sin[2\kappa h]}, & |y| < h \\ E_z(q, -h, \zeta, s) \exp[i\kappa(y + h)], & y < -h \end{cases} \quad (4)$$

where  $\kappa^2 = q^2 - p^2$ . The branch for  $\kappa$  in the complex  $q$ -plane is so chosen that  $\text{Im}\{\kappa\} \leq 0$  in that branch. It now remains to determine  $E_z(q, \pm h, \zeta, s)$  from the boundary conditions at  $y = \pm h$ , namely that  $E_z(x, \pm h, \zeta, s) = 0$  for  $|x| < w$ , and that  $(\partial/\partial y) E_z(x, \pm h, \zeta, s)$  is continuous for  $|x| > w$ . For that reason one splits the unknown function  $\tilde{E}_z(q, y, \zeta, s)$  in the following way:

$$E_z(q, y, \zeta, s) = E_+(q, y) + E_-(q, y) + E_1(q, y) \quad (5)$$

such that

$$\begin{aligned} \frac{1}{2\pi i} \int_C E_-(q, y) \exp(qx) dq &= \begin{cases} E_z(x, y, s, \zeta), & x < -w \\ 0, & x > -w \end{cases} \\ \frac{1}{2\pi i} \int_C E_+(q, y) \exp(qx) dq &= \begin{cases} 0, & x < w \\ E_z(x, y, s, \zeta), & x > w \end{cases} \\ \frac{1}{2\pi i} \int_C E_1(q, y) \exp(qx) dq &= \begin{cases} 0, & |x| > w \\ E_z(x, y, s, \zeta), & |x| < w. \end{cases} \end{aligned} \quad (6)$$

From these integrals it is immediately seen that  $E_+(q,y)$  is a holomorphic function of  $q$  to the right of  $C$ , that  $E_-(q,y)$  is a holomorphic function of  $q$  to the left of  $C$ , and that  $E_1(q,y)$  is an entire function of  $q$ . By invoking the boundary condition that  $(\partial/\partial y)E_z$  is continuous at  $y = \pm h$ ,  $|x| > w$  one obtains the following two relationships,

$$E_1'(q, \pm h+) - E_1'(q, \pm h-) = -\kappa[i + \cot(2\kappa h)][E_+(q, \pm h) + E_-(q, \pm h) + E_1(q, \pm h)] \\ + \kappa \csc(2\kappa h)[E_+(q, \mp h) + E_-(q, \mp h) + E_1(q, \mp h)] \quad (7)$$

where the prime denotes differentiation with respect to the second argument of  $E_1(q,y)$ . Addition and subtraction of these two equations result in the following equations:

$$\tilde{u}_s(q) = K(q)\tilde{e}_s(q) \\ \tilde{u}_a(q) = L(q)\tilde{e}_a(q) \quad (8)$$

where

$$\tilde{u}_s(q) = E_1'(q, h-) - E_1'(q, h+) + E_1'(q, -h-) - E_1'(q, -h+) \\ \tilde{u}_a(q) = E_1'(q, h-) - E_1'(q, h+) - E_1'(q, -h-) + E_1'(q, -h+) \\ \tilde{e}_s(q) = E_+(q, h) + E_-(q, h) + E_1(q, h) + E_+(q, -h) + E_-(q, -h) + E_1(q, -h) \\ \tilde{e}_a(q) = E_+(q, h) + E_-(q, h) + E_1(q, h) - E_+(q, -h) - E_-(q, -h) - E_1(q, -h) \\ K(q) = \kappa[i + \cot(2\kappa h) - \csc(2\kappa h)] = i\kappa \sec(\kappa h)\exp(i\kappa h) \\ L(q) = \kappa[i + \cot(2\kappa h) + \csc(2\kappa h)] = \kappa \csc(\kappa h)\exp(i\kappa h). \quad (9)$$

Note that  $\tilde{u}_s$  and  $\tilde{u}_a$  are related to  $u_-$  and  $u_+$  in [6] via

$$u_+(x) = \frac{1}{2\pi i} \int_C \tilde{u}_s(q) \exp(qx) dq \quad (10)$$

$$u_-(x) = \frac{1}{2\pi i} \int_C \tilde{u}_a(q) \exp(qx) dq$$

and that  $\tilde{u}_s(\tilde{u}_a)$  corresponds to the case where the longitudinal currents have the same magnitude and the same (opposite) direction on the two plates. These two different cases have been referred to as the symmetric and antisymmetric cases, respectively.

The so-called Jones' version<sup>[10,11]</sup> of the method of Wiener and Hopf will now be used to solve the two equations in (8), i.e., find  $E_{\pm}(q, \pm h)$  and  $E'_1(q, \pm h)$ . Note that  $E'_{\pm}(q, \pm h+) - E'_{\pm}(q, \pm h-) = 0$  and that  $E_1(q, \pm h)$  is given by the incident field. The method starts out with splitting the "kernel function"  $K(q)$  in the following way:

$$K(q) = K_+(q)/K_-(q) \quad (11)$$

$$K_+(q)K_-(-q) = -1$$

such that  $K_+(q)$  is holomorphic to the right of the path of integration  $C$  in (6) and  $K_-(q)$  is holomorphic to the left of  $C$ . By choosing  $C$  as shown in Fig. 3 one can find an infinite product representation of  $K_+(q)$  ( $\gamma = 0.577\dots$ )

$$K_+(q) = \frac{i(q+p)^{1/2} \exp\left\{(\kappa h/\pi) \ln[(q+\kappa)/p] + (qh/\pi) \ln[(\pi/2ph) - \gamma + 1]\right\}}{\prod_{m=0}^{\infty} [(q+\kappa)_{2m+1} 2h/(2m+1)\pi] \exp[-2qh/(2m+1)\pi]} \quad (12)$$

Before substituting (11) for  $K(q)$  into (8) it is noted that asymptotically for large values of  $|q|$  one has

$$K_+(q) \sim i\sqrt{2(p+q)} + O(q^{-1} \ln q), \quad |q| \rightarrow \infty \text{ to the right of } C$$

and

$$K_-(q) \sim i/\sqrt{2(p-q)} + O(q^{-3/2} \ln q), \quad |q| \rightarrow \infty \text{ to the left of } C. \quad (13)$$

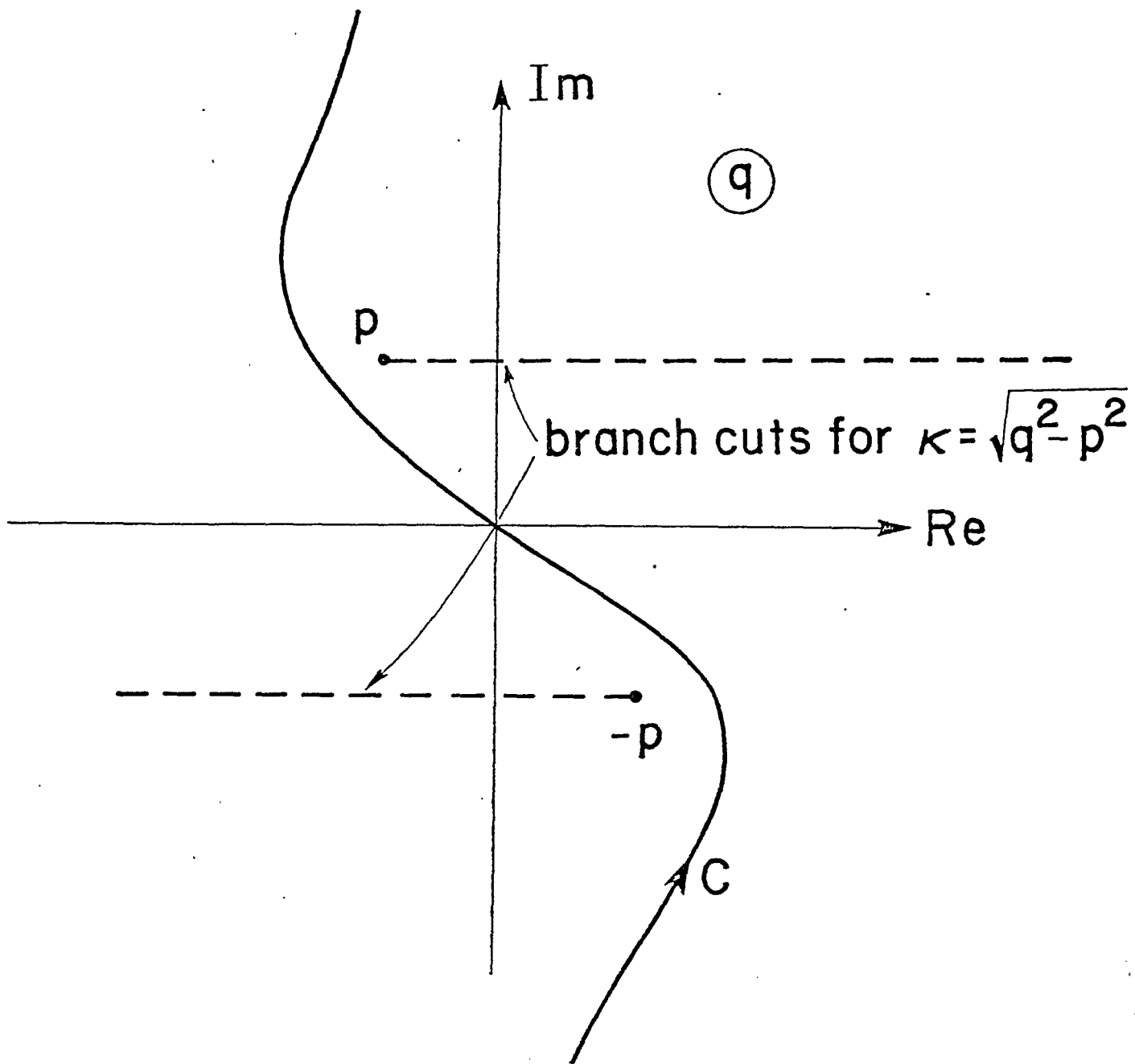


Figure 3. The path of integration  $C$  in the inverse Laplace transform integral.

The boundary conditions on the plate also imply that

$$\begin{aligned} E_1(q, \pm h) &= \int_{-w}^w E_z(x, \pm h, \zeta, s) \exp(-qx) dx \\ &= - \int_{-w}^w E_z^{\text{inc}}(x, \pm h, \zeta, s) \exp(-qx) dx \end{aligned} \quad (14)$$

and since  $E_z^{\text{inc}}$  is finite on the plates it is clear that

$$E_1(q, \pm h) \sim \exp(qw), \quad |q| \rightarrow \infty, \quad \text{Re}\{q\} > 0 \quad (15)$$

$$E_1(q, \pm h) \sim \exp(-qw), \quad |q| \rightarrow \infty, \quad \text{Re}\{q\} < 0.$$

In view of (9) and (11) it is useful to rewrite (8) as

$$K_-(q) \exp(qw) \tilde{u}_s(q) = K_+(q) \exp(qw) [\chi_+(q) + \chi_-(q) + \chi_1(q)] \quad (16)$$

where

$$\chi_{\pm}(q) = E_{\pm}(q, h) + E_{\pm}(q, -h), \quad \chi_1(q) = E_1(q, h) + E_1(q, -h) \quad (17)$$

and  $\chi_1(q)$  is solely determined by the incident field, (c.f. (9)). The term  $K_+(q) \exp(qw) \chi_+(q)$  in (16) is a holomorphic function to the right of  $C$  and the remaining term,  $X(q)$  in (16) can be split into the sum of two terms, one of these terms,  $X_+(q)$ , being holomorphic to the right of  $C$  and the other term,  $X_-(q)$ , being holomorphic to the left of  $C$ , thereby yielding

$$X(q) \equiv K_+(q) \exp(qw) [\chi_-(q) + \chi_1(q)] = X_+(q) + X_-(q) \quad (18)$$

where

$$X_+(q) = - \frac{1}{2\pi i} \int_C \frac{K_+(q') \exp(q'w) [\chi_-(q') + \chi_1(q')]}{q' - q} dq' \quad (19)$$

$$X_-(q) = -1/X_+(-q).$$

Thus, (8) can be rearranged as

$$K_+(q)\exp(qw)\tilde{u}_s(q) - X_-(q) = K_+(q)\exp(qw)\chi_+(q) + X_+(q). \quad (20)$$

By the standard argument each side of (20) is an entire function of  $q$  and from the edge conditions it can be seen that each side tends to zero as  $q$  tends to infinity in their respective half space of holomorphicity. Therefore, each side is identically zero for all values of  $q$ , so that one gets

$$K_+(q)\exp(qw)\chi_+(q) = -X_+(q). \quad (21)$$

In this equation both  $\chi_+(q)$  and  $X_+(q)$  are unknown. To find the unknowns  $\chi_{\pm}(q)$  of (21) it is advantageous first to go back to (8) and rewrite that equation in the following way:

$$K_+^{-1}(q)\exp(-qw)\tilde{u}_s(q) - Y_+(q) = K_-^{-1}(q)\exp(-qw)\chi_-(q) + Y_-(q) \quad (22)$$

where  $Y_+(q)$  and  $Y_-(q)$  are the parts of  $Y(q)$  which are holomorphic to the right and left of  $C$ , respectively, (c.f. (18)) and

$$Y_+(q) + Y_-(q) = Y(q) = K_-^{-1}(q)\exp(-qw)[\chi_+(q) + \chi_-(q)]. \quad (23)$$

Again, by the standard argument in the Wiener-Hopf method and from the edge conditions at  $x = \pm w$  one gets

$$K_-^{-1}(-q)\exp(qw)\chi_-(-q) = -Y_-(-q). \quad (24)$$

Equations (21) and (24) have the same domain of analyticity, i.e., both sides of these equations are holomorphic functions of  $q$  to the right of  $C$ . From (18) and (23) it is also obvious that (21) and (24) form a set of two coupled integral equations for  $\chi_{\pm}(q)$ . These two equations can be reduced to two uncoupled integral equations by adding and subtracting (21) and (24) to each other thereby yielding

$$K_+(q)\tilde{x}_s^e(q) - \frac{1}{2\pi i} \int_C \frac{\exp(-2q'w)\tilde{x}_s^e(q')}{(q'+q)K_-(q')} dq' = \frac{1}{2\pi i} \int_C \frac{[\chi_1(q')+\chi_1(-q')] \exp(-q'w)}{(q'+q)K_-(q')} dq' \quad (25)$$

$$K_-(q)\tilde{x}_s^o(q) + \frac{1}{2\pi i} \int_C \frac{\exp(-2q'w)\tilde{x}_s^o(q')}{(q'+q)K_-(q')} dq' = \frac{1}{2\pi i} \int_C \frac{[\chi_1(-q')-\chi_1(q')] \exp(-q'w)}{(q'+q)K_-(q')} dq'$$

where

$$\tilde{x}_s^e(q) = [\chi_+(q) + \chi_-(-q)] \exp(qw) \quad (26)$$

$$\tilde{x}_s^o(q) = [\chi_+(q) - \chi_-(-q)] \exp(qw).$$

The solutions  $\tilde{x}_s^e$  and  $\tilde{x}_s^o$  can be interpreted in the following way: from the symmetry of the problem it is evident that  $E_z$  can be separated into a symmetric part  $E_{zs}$  and an antisymmetric part  $E_{za}$  such that

$$E_{zs}(x,y,\zeta,s) = \frac{1}{2} [E_z(x,y,\zeta,s) + E_z(x,-y,\zeta,s)] \quad (27)$$

$$E_{za}(x,y,\zeta,s) = \frac{1}{2} [E_z(x,y,\zeta,s) - E_z(x,-y,\zeta,s)].$$

Each one of these parts can be split into its even and odd parts such that

$$E_{zs}^e(x,y,\zeta,s) = \frac{1}{2} [E_{zs}(x,y,\zeta,s) + E_{zs}(-x,y,\zeta,s)] \quad (28)$$

$$E_{zs}^o(x,y,\zeta,s) = \frac{1}{2} [E_{zs}(x,y,\zeta,s) - E_{zs}(-x,y,\zeta,s)]$$

and similarly for  $E_{za}$ . From (26), (27) and (28) one then sees that an inverse Laplace transform integral of  $\tilde{x}_s^e(q)\exp(-qw)$  gives  $E_{zs}^e(x,h,\zeta,s)$  and that an inverse Laplace transform integral of  $\tilde{x}_s^o(q)\exp(-qw)$  gives  $E_{zs}^o(x,h,\zeta,s)$ . Thus, the solutions of (25) determine the even and odd parts of the symmetric, transverse magnetic field.

In the next section a method of solving (25) will be discussed. However, before doing so it is advantageous first to derive a set of integral equations for the antisymmetric part of the TM field. Going back to the second equation in (8) and following the steps in deriving the integral equations (25) one

first splits  $L(q)$  such that

$$L(q) = L_+(q)/L_-(q) \quad (29)$$

$$L_+(q)L_-(-q) = -1$$

and

$$L_+(q) = \frac{i\sqrt{2} \exp\{(\kappa h/\pi)\ln[(q+\kappa)/p] + (qh/\pi)\ln[(\pi/2ph) - \gamma + 1]\}}{\prod_{m=1}^{\infty} [(q+\kappa)_{2m} h/m\pi] \exp[-qh/m\pi]}$$

The functions  $L_+(q)$  and  $L_-(q)$  have properties similar to those of  $K_+(q)$  and  $K_-(q)$ , the asymptotic behavior being the same. Therefore, an analysis similar to the one leading up to (25) results in the following set of integral equations:

$$L_+(q)\tilde{x}_a^e(q) - \frac{1}{2\pi i} \int_C \frac{\exp(-2q'w)\tilde{x}_a^e(q')}{(q'+q)L_-(q')} dq' = \frac{1}{2\pi i} \int_C \frac{[\lambda_1(q') + \lambda_1(-q')] \exp(-q'w)}{(q'+q)L_-(q')} dq' \quad (30)$$

$$L_-(q)\tilde{x}_a^o(q) + \frac{1}{2\pi i} \int_C \frac{\exp(-2q'w)\tilde{x}_a^o(q')}{(q'+q)L_-(q')} dq' = \frac{1}{2\pi i} \int_C \frac{[\lambda_1(-q') - \lambda_1(q')] \exp(-q'w)}{(q'+q)L_-(q')} dq'$$

where

$$\begin{aligned} \tilde{x}_a^e(q) &= [E_+(q,h) - E_+(q,-h) + E_-(-q,h) - E_-(-q,h)] \exp(qw) \\ \tilde{x}_a^o(q) &= [E_+(q,h) - E_+(q,-h) - E_-(-q,h) + E_-(-q,-h)] \exp(qw) \end{aligned} \quad (31)$$

$$\lambda_1(q) = E_1(q,h) - E_1(-q,-h).$$

The solutions of (30) determine all the properties of the antisymmetric part of the transverse magnetic field.

## B. Transverse Electric Fields

Having derived integral equations the solutions of which give the transverse magnetic field it now remains to derive equations governing the

transverse electric field. As is well known the TE-field is uniquely determined by the  $H_z$  component, which satisfies the differential equation off the plates,

$$\left[ \frac{\partial^2}{\partial x^2} + \frac{\partial^2}{\partial y^2} - p^2 \right] H_z = 0. \quad (32)$$

Following the same approach as the one used for determining  $E_z$  one puts

$$H_z(x, y, \zeta, s) = \frac{1}{2\pi i} \int_C \tilde{H}_z(q, y, \zeta, s) \exp(qx) dq. \quad (33)$$

The fact that  $\tilde{H}_z$  satisfies the ordinary differential equation

$$\left[ \frac{d^2}{dy^2} + \kappa^2 \right] \tilde{H}_z = 0 \quad (34)$$

together with the outgoing wave condition for  $\tilde{H}_z(q, y, \zeta, s)$  as  $|y| \rightarrow \infty$  and  $(\partial/\partial y)H_z$  being continuous at  $y = \pm h$  (since  $E_x$  is continuous at  $y = \pm h$ ) results in the following representation for  $\tilde{H}_z$ :

$$\tilde{H}_z(q, y, s, \zeta) = \begin{cases} (i\kappa)^{-1} F(q, h) \exp[-i\kappa(y - h)], & y > h \\ \kappa^{-1} F(q, h) \frac{\cos[\kappa(y+h)]}{\sin[2\kappa h]} + \kappa^{-1} F(q, -h) \frac{\cos[\kappa(y-h)]}{\sin[2\kappa h]}, & |y| < h \\ (i\kappa)^{-1} F(q, -h) \exp[i\kappa(y + h)], & y < -h. \end{cases} \quad (35)$$

It is to be noted that  $F(q, \pm h)$  is proportional to  $\tilde{E}_x(q, \pm h, s, \zeta)$ . Splitting  $\tilde{H}_z(q, y, s, \zeta)$  and  $F(q, y)$  into three parts as has been done in (6),

$$\tilde{H}_z(q, y, s, \zeta) = H_+(q, y) + H_-(q, y) + H_1(q, y) \quad (36)$$

$$F(q, y) = F_+(q, y) + F_-(q, y) + F_1(q, y)$$

and using the boundary condition that  $H_z(x, y, \zeta, s)$  is continuous at  $y = \pm h$  and  $|x| > w$  one gets

$$\begin{aligned}
H_1(q, \pm h+) - H_1(q, \pm h-) &= \mp \kappa^{-1} [i + \cot(2\kappa h)] [F_+(q, \pm h) + F_-(q, \pm h) + F_1(q, \pm h)] \\
&\mp \kappa^{-1} \csc(2\kappa h) [F_+(q, \mp h) + F_-(q, \mp h) + F_1(q, \mp h)]. \quad (37)
\end{aligned}$$

By adding and subtracting these two equations and noting that  $F_1(q, \pm h) = 0$  one obtains the following set of two equations:

$$\begin{aligned}
\tilde{v}_s(q) &= P(q) f_s(q) \\
\tilde{v}_a(q) &= Q(q) f_a(q)
\end{aligned} \quad (38)$$

where

$$\begin{aligned}
\tilde{v}_s(q) &= -H_1(q, h+) + H_1(q, h-) - H_1(q, -h+) + H_1(q, -h-) \\
\tilde{v}_a(q) &= -H_1(q, h+) + H_1(q, h-) + H_1(q, -h+) - H_1(q, -h-) \\
f_s(q) &= F(q, h) - F(q, -h) \\
f_a(q) &= F(q, h) + F(q, -h) \\
P(q) &= \kappa^{-1} [i + \cot(2\kappa h) + \csc(2\kappa h)] = L(q)/\kappa^2 \\
Q(q) &= \kappa^{-1} [i + \cot(2\kappa h) - \csc(2\kappa h)] = K(q)/\kappa^2.
\end{aligned} \quad (39)$$

It should be pointed out that  $\tilde{v}_s$  is related to  $v_+$  in [6] via

$$p^2 v_+(x) / s\mu_0 = \frac{1}{2\pi i} \int_C \tilde{v}_s(q) \exp(qx) dq \quad (40)$$

and similarly for  $\tilde{v}_a$  and  $v_-(x)$ . Also,  $\tilde{v}_s$  ( $\tilde{v}_a$ ) corresponds to the case where the longitudinal currents have the same magnitude and the same (opposite) direction on the two plates. From (35) and (39) it is also clear that  $\tilde{v}_s$  ( $\tilde{v}_a$ ) gives rise to an electromagnetic field where  $H_z$  is an even (odd) function of  $y$ .

To find  $\tilde{v}_s$  and  $\tilde{v}_a$  the same approach will be followed as the one used in determining the transverse magnetic field. For that reason, define the quantities

$$\phi_{\pm}(q) = F_{\pm}(q, h) + F_{\pm}(q, -h), \quad \phi_1(q) = F_1(q, h) + F_1(q, -h) \quad (41)$$

and  $\phi_1(q)$  is uniquely determined by the incident field since the boundary conditions on the plates require that the x-component of the total field be zero on the plates implying that

$$\begin{aligned} F_1(q, \pm h) &= (s\mu_0)^{-1} \int_{-w}^w E_x(x, \pm h, \zeta, s) \exp(-qx) dx \\ &= -(s\mu_0)^{-1} \int_{-w}^w E_x^{\text{inc}}(x, \pm h, \zeta, s) \exp(-qx) dx. \end{aligned} \quad (42)$$

Instead of deriving integral equations for  $\phi_{\pm}(q)$  it is advantageous to introduce the even and odd parts of these two functions,

$$\tilde{y}_s^e(q) = [\phi_+(q) - \phi_-(-q)] \exp(qw) \quad (43)$$

$$\tilde{y}_s^o(q) = [\phi_+(q) + \phi_-(-q)] \exp(qw) .$$

The function  $\tilde{y}_s^e(q)$  ( $\tilde{y}_s^o(q)$ ) corresponds to the case where the longitudinal current distribution on each plate is an even (odd) function with respect to the plate's center line. Following the Jones version of the Wiener-Hopf method one obtains the following two uncoupled integral equations for  $\tilde{y}_s^e$  and  $\tilde{y}_s^o$ ,

$$P_+(q) \tilde{y}_s^e(q) - \frac{1}{2\pi i} \int_C \frac{\exp(-2q'w) \tilde{y}_s^e(q')}{(q'+q)P_-(q')} dq' = \frac{1}{2\pi i} \int_C \frac{[\phi_1(q') + \phi_1(-q')] \exp(-q'w)}{(q'+q)P_-(q')} dq' \quad (44)$$

$$P_+(q) \tilde{y}_s^o(q) + \frac{1}{2\pi i} \int_C \frac{\exp(-2q'w) \tilde{y}_s^o(q')}{(q'+q)P_-(q')} dq' = \frac{1}{2\pi i} \int_C \frac{[\phi_1(-q') - \phi_1(q')] \exp(-q'w)}{(q'+q)P_-(q')} dq'$$

where

$$P_+(q) = L_+(q)/(q + p) \quad (45)$$

$$P_-(q) = (q - p)L_-(q).$$

The solution of (44) determines the even and odd parts of the symmetric part of the transverse electric field.

It now remains to derive integral equations for the even and odd parts of the antisymmetric part of the transverse electric field. This is done by introducing the quantities

$$\tilde{y}_a^e(q) = [\psi_+(q) - \psi_-(q)] \exp(qw) \quad (46)$$

$$\tilde{y}_a^o(q) = [\psi_+(q) + \psi_-(q)] \exp(qw)$$

where

$$\psi_{\pm}(q) = F_{\pm}(q, h) - F_{\pm}(q, -h) \quad (47)$$

and one immediately obtains the two integral equations

$$Q_+(q) \tilde{y}_a^e(q) - \frac{1}{2\pi i} \int_C \frac{\exp(-2q'w) \tilde{y}_a^e(q')}{(q'+q)Q_-(q')} dq' = \frac{1}{2\pi i} \int_C \frac{[\psi_1(q') + \psi_1(-q')] \exp(-q'w)}{(q'+q)Q_-(q')} dq' \quad (48)$$

$$Q_+(q) \tilde{y}_a^o(q) + \frac{1}{2\pi i} \int_C \frac{\exp(-2q'w) \tilde{y}_a^o(q')}{(q'+q)Q_-(q')} dq' = \frac{1}{2\pi i} \int_C \frac{[\psi_1(-q') - \psi_1(q')] \exp(-q'w)}{(q'+q)Q_-(q')} dq'$$

where

$$\psi_1(q) = F_1(q, h) - F_1(q, -h)$$

$$Q_+(q) = K_+(q)/(q + p)$$

$$Q_-(q) = (q - p)K_-(q). \quad (49)$$

To sum up this section, integral equations for the field scattered from

two parallel plates of finite width have been derived. It was found that the most natural decomposition of the field is to use (1) its transverse electric and transverse magnetic parts (2) its symmetric and antisymmetric parts (referring to the symmetry of the electromagnetic field in the direction perpendicular to the plates) and (3) its even and odd parts (referring to the symmetry of the electromagnetic field in the transverse direction parallel to the plates). In each one of these cases (which together combine to eight different independent cases) a scalar integral equation of the second kind was derived.

Although the equations derived here are exact, they are most useful for numerical treatment only when the width of the plates is large compared to the plate separation. Therefore, they complement the integral equations derived in a previous note. In the next section the integral equations derived in this note will be used to find properties of the lowest-order TM modes and TE modes for two wide plates.

### III. Transverse Propagation Constants of Modes on Two Wide Plates

The integral equations derived in the previous section will now be used to calculate the transverse propagation constants of the TM and TE modes on two wide parallel plates. These quantities are of course determined from the non-trivial solutions of the homogeneous equations (25), (30), (44), and (48).

#### A. Even, Symmetric TM Modes

The homogeneous integral equation for the even, symmetric TM field is

$$K_+(q)\tilde{x}_s^e(q) - \frac{1}{2\pi i} \int_C \frac{\exp(-2q'w)\tilde{x}_s^e(q')}{(q'+q)K_-(q')} dq' = 0 \quad (50)$$

where  $q$  is "to the left" of  $C$  (c.f. Fig. 3). By changing the path of integration to  $C_1$  one obtains

$$K_+(q)\tilde{x}_s^e(q) + K_+(q)\exp(2qw)\tilde{x}_s^e(-q') - \frac{1}{2\pi i} \int_C \frac{\exp(-2q'w)\tilde{x}_s^e(q')}{(q'+q)K_-(q')} dq' = 0. \quad (51)$$

Equation (50) holds for  $q$  lying to the left of  $C$ , whereas (51) holds for  $q$  lying to the right of  $C_1$ . By comparing (50) and (51) one finds that  $\tilde{x}_s^e(q)$  has a branch cut at  $q = -p$ . Furthermore, the integrand tends to zero as  $q' \rightarrow \infty$  in the right half plane so that the path of integration in (50) can be deformed to the right, resulting in the following expression:

$$K_+(q)\tilde{x}_s^{(e)}(q) + \sum_{m=0}^{\infty} \frac{\exp(-2w\kappa_{2m+1})\tilde{x}_s^e(\kappa_{2m+1})}{(q+\kappa_{2m+1})K'_-(\kappa_{2m+1})} - \frac{1}{2\pi i} \int_{C_2} \frac{\exp(-2q'w)\tilde{x}_s^e(q')}{(q'+q)K_-(q')} dq' = 0 \quad (52)$$

where

$$\kappa_n = \sqrt{(n\pi/2h)^2 + p^2},$$

the prime denotes differentiation and the path of integration  $C_2$  is shown in Fig. 4. Since  $\tilde{x}_s^{(e)}(q)$  is a holomorphic function on  $C_2$ , (52) can be used to formulate an integral equation for  $\tilde{x}_s^{(e)}(q)$  when  $q$  belongs to  $C_2$ . Once this solution is known (52) determines  $\tilde{x}_s^e(q)$  for arbitrary complex values of  $q$ .

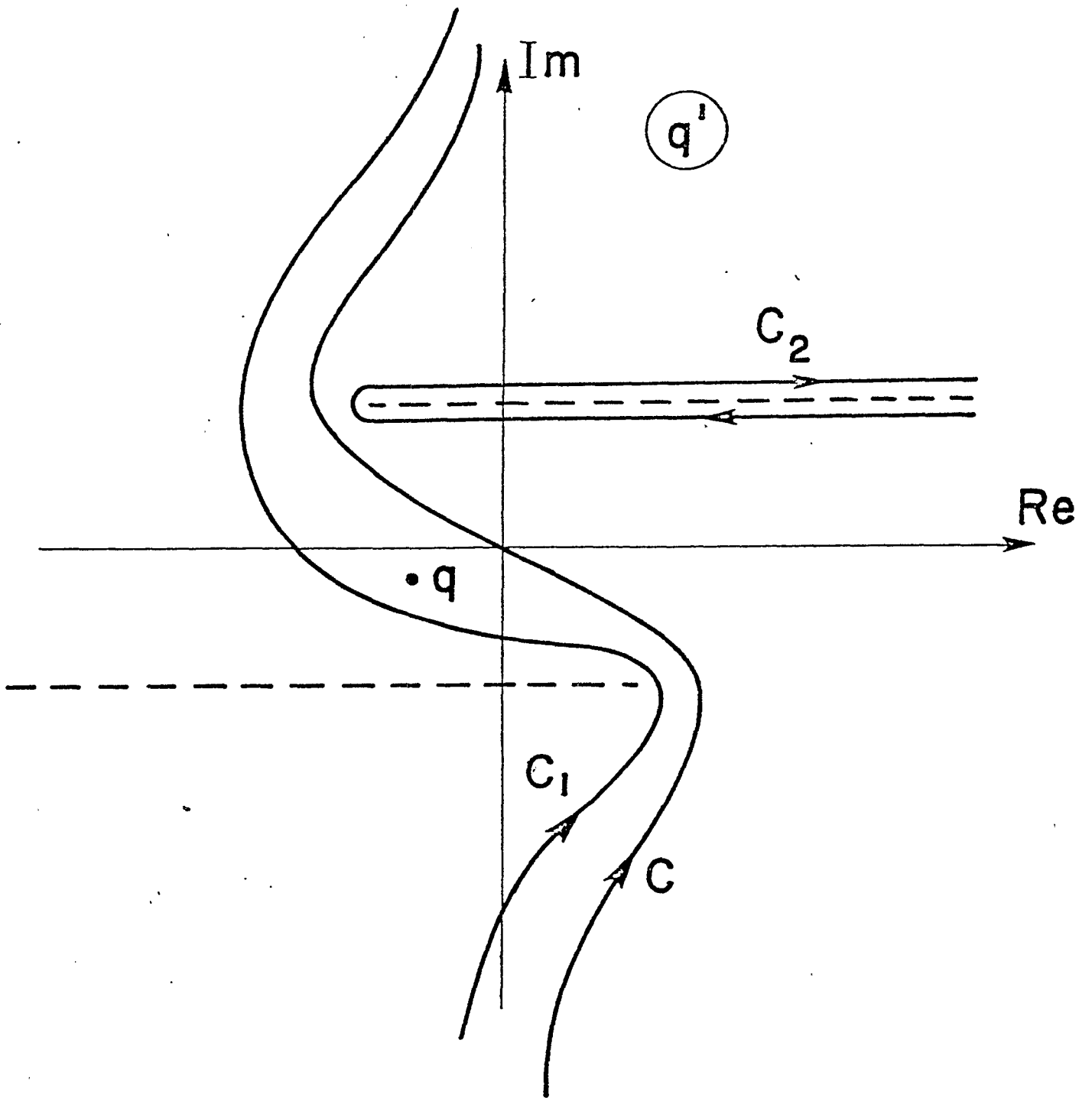


Figure 4. The paths of integration  $C$ ,  $C_1$ , and  $C_2$  in the complex  $q'$  plane.

In the general case, (52) must be "solved" using numerical techniques. However, it can also be used to find an analytical expression for the transverse propagation constant in some limiting cases. Consider the case where  $\pi/h \gg |p|$  so that each term of the sum in (52) is exponentially small. In this case the entire sum is negligible and one, therefore, has the following approximate integral equation:

$$K_+(q)\tilde{x}_s^e(q) - \frac{1}{2\pi i} \int_{C_2} \frac{\exp(-2q'w)\tilde{x}_s^e(q')}{(q'+q)K_-(q')} dq' = 0, \quad q \in C_2 \quad (53)$$

which can be cast into the alternative form,

$$M(\xi)h_s^e(\xi) - \int_0^\infty \frac{\exp(-2\xi'w)h_s^e(\xi')}{2p + \xi + \xi'} d\xi' = 0, \quad 0 \leq \xi < \infty \quad (54)$$

where

$$h_s^e(\xi) = k(\xi)\tilde{x}_s^e(p + \xi)$$

$$M(\xi) = 2\pi i \exp(2pw)K_+(p + \xi)/k(\xi)$$

and

$$k(\xi) = \lim_{\epsilon \rightarrow 0^+} \left[ \frac{1}{K_-(p + \xi + i\epsilon)} - \frac{1}{K_-(p + \xi - i\epsilon)} \right] \quad (55)$$

i.e.,  $k(\xi)$  is the discontinuity of  $K_-^{-1}(q)$  across the branch cut.

For large values of  $|pw|$  the main contribution to the integral comes from small values of  $\xi'$ . By using a small argument approximation of  $M(\xi)$  one gets

$$\pi\sqrt{2p/\xi} \exp(2pw)h_s^e(\xi) - \int_0^\infty \frac{\exp(-2\xi'w)h_s^e(\xi')}{2p + \xi + \xi'} d\xi' = 0. \quad (56)$$

The integral defines a function of  $\xi$  which is analytic at  $\xi = 0$  provided that  $h_s^e(\xi)$  satisfies certain requirements for large values of  $\xi$  so that the integral exists. For small values of  $\xi$  one therefore has approximately

$$h_s^e(\xi) \approx h_s^e \sqrt{\xi} \quad (57)$$

resulting in the following equation

$$h_s^e \left[ \pi \sqrt{2p} \exp(2pw) - \int_0^\infty \frac{\sqrt{\xi'} \exp(-2\xi'w)}{2p + \xi'} d\xi' \right] = 0 \quad (58)$$

When  $|pw|$  is not small one has

$$h_s^e \left[ \pi (2p)^{3/2} \exp(2pw) - \int_0^\infty \sqrt{\xi'} \exp(-2\xi'w) d\xi' \right] = 0 \quad (59)$$

For this equation to have a nontrivial solution, i.e.,  $h_s^e \neq 0$ ,  $p$  must satisfy the equation

$$16\sqrt{\pi} (pw)^{3/2} \exp(2pw) - 1 = 0. \quad (60)$$

For large values of  $|pw|$  this equation has the asymptotic solution

$$p_{s,n}^e w = \left(n - \frac{3}{8}\right) \pi i - \frac{1}{4} \ln(256\pi^4 n^3) + O(n^{-1} \ln n) \quad (61)$$

In the general case (60) must be solved numerically and the results of the numerical calculations are shown in Fig. 5. It was found that the asymptotic form (61) agrees within 10% with the exact solution of (60) except for the lowest root ( $n = 1$ ). The field distribution of this mode will be investigated in the next section, showing that the field of this mode is very weak between the plates.

#### B. Odd, Symmetric TM Modes

For the odd, symmetric TM field one gets, with the same procedure as above

$$h_s^o(\xi) \approx h_s^o \sqrt{\xi} \quad (62)$$

and

$$h_s^o \left[ \pi (2p)^{3/2} \exp(2pw) + \int_0^\infty \sqrt{\xi'} \exp(-2\xi'w) d\xi' \right] = 0 \quad (63)$$

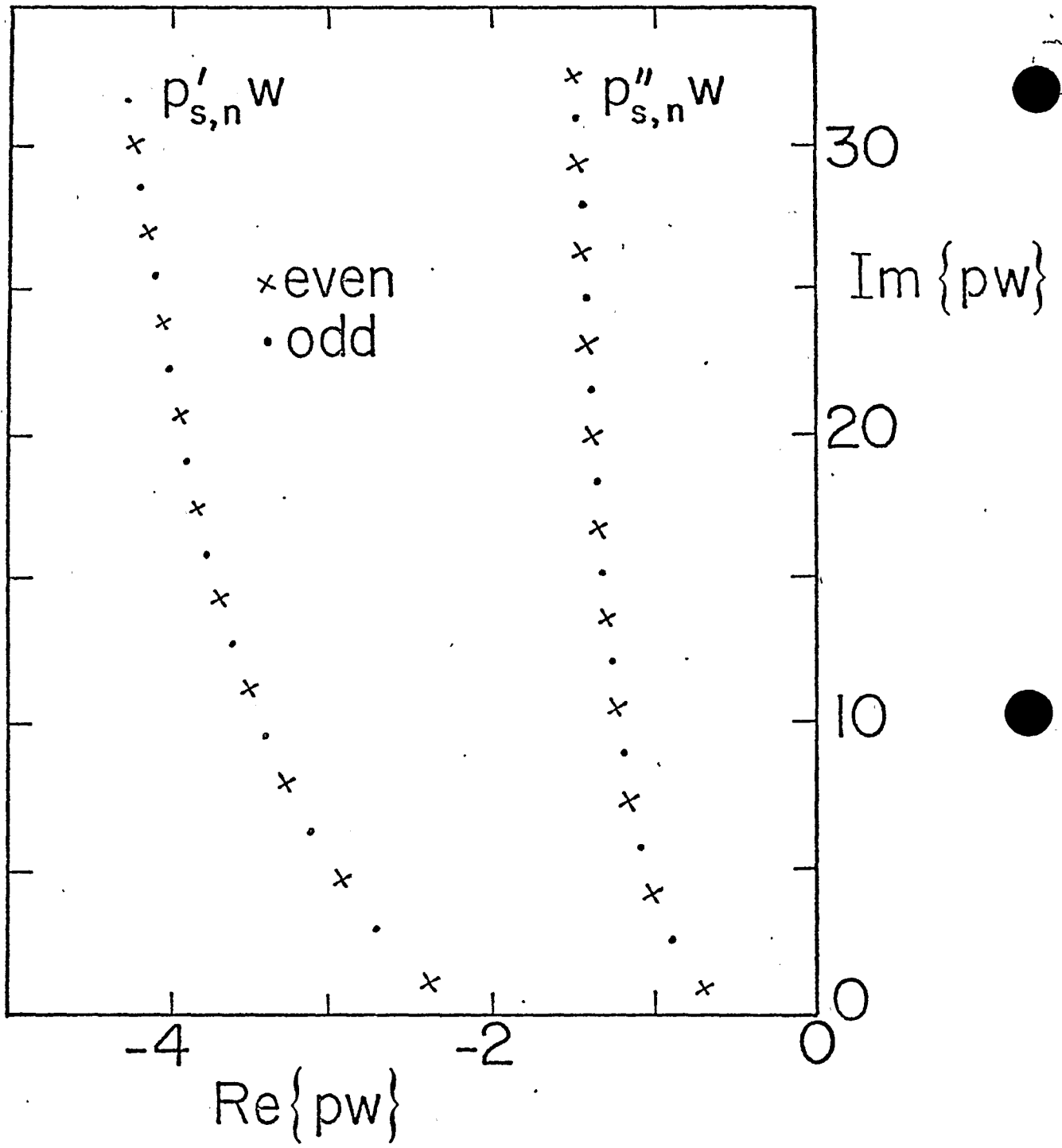


Figure 5. The transverse propagation constants for the symmetric TM modes ( $p'_{s,n}$ ) and the symmetric TE modes ( $p''_{s,n}$ ).

which has nontrivial solutions when  $p$  satisfies the equation

$$16\sqrt{\pi} (pw)^{3/2} \exp(2pw) + 1 = 0 \quad (64)$$

Again, the roots of this transcendental equation can be found using numerical techniques (see Fig. 5) and for large values of  $|pw|$  one has asymptotically

$$p_{s,n}^{1,0} w = (n + \frac{1}{8})\pi i - \frac{1}{4} \ln(256\pi^4 n^3) + o(n^{-1} \ln n) \quad (65)$$

### C. Even, Antisymmetric TM Modes

The even, antisymmetric TM modes are determined from the integral equation

$$L_+(q)\tilde{x}_a^e(q) - \frac{1}{2\pi i} \int_C \frac{\exp(-2q'w)\tilde{x}_a^e(q')}{(q'+q)L_-(q')} dq' = 0, \quad q \in C \quad (66)$$

which can also be written in the following form

$$N(\xi)h_a^e(\xi) - \int_0^\infty \frac{\exp(-2\xi'w)h_a^e(\xi')}{2p + \xi + \xi'} d\xi' = 0, \quad 0 < \xi < \infty \quad (67)$$

where

$$h_a^e(\xi) = \ell(\xi)\tilde{x}_a^e(p + \xi)$$

$$N(\xi) = 2\pi i \exp(2pw)L_+(p + \xi)/\ell(\xi)$$

and

$$\ell(\xi) = \lim_{\epsilon \rightarrow 0^+} \left[ \frac{1}{L_-(p + \xi + i\epsilon)} - \frac{1}{L_-(p + \xi - i\epsilon)} \right] \quad (68)$$

For large values of  $|pw|$  one can use the same type of approximations as those employed in (54) to obtain the following approximate equations

$$h_a^e(\xi) \approx h_a^e \sqrt{\xi} \quad (69)$$

$$h_a^e \left[ \frac{\pi}{h} \sqrt{2p} \exp \left\{ 2pw + (2ph/\pi) \left[ \ln(2\pi/ph) - \gamma + 1 - i\pi/2 \right] \right\} - \int_0^\infty \sqrt{\xi'} \exp(-2\xi'w) d\xi' \right] = 0$$

In order for  $h_a^e$  not to be zero  $p$  must be a root of the transcendental equation

$$8\sqrt{\pi p w^3/h^2} \exp \left\{ 2pw + (2ph/\pi) \left[ \ln(2\pi/ph) - \gamma + 1 \right] \right\} - 1 = 0 \quad (70)$$

Before trying to solve this equation, it should be pointed out that it has been derived under the assumption that  $|ph| \ll 1$ . Thus, the roots of interest of (70) must therefore satisfy  $|ph| \ll 1$ . The roots  $p_{a,n}^e$  of (70) were found numerically using a desk calculator and they are presented in Fig. 6 for different values of  $w/h$ .

#### D. Odd, Antisymmetric TM Modes

Similarly, the transverse propagation constant  $p_{s,n}^o$  of the odd, antisymmetric modes are determined by the solutions of the equation

$$8\sqrt{\pi p w^3/h^2} \exp \left\{ 2pw + (2ph/\pi) \left[ \ln(2\pi/ph) - \gamma + 1 \right] \right\} + 1 = 0 \quad (71)$$

and they are shown in Fig. 6. Again, it is found that the absolute value of the real part of the propagation constants gets larger as  $h/w$  gets smaller. This effect can be understood from the fact that the field of this mode is mainly outside the two plates.

#### E. Even, Symmetric TE Modes

Turning the attention to the transverse electric field one has the following integral equation determining the even, symmetric TE modes,

$$P_+(q) \tilde{y}_s^e(q) - \sum_{m=0}^{\infty} \frac{\exp(-2w\kappa_{2m+1}) \tilde{y}_s^e(\kappa_{2m+1})}{(q+\kappa_{2m+1}) P_-(\kappa_{2m+1})} + \frac{1}{2\pi i} \int_{C_2} \frac{\exp(-2q'w) \tilde{y}_s^e(q')}{(q'+q) P_-(q')} dq' = 0 \quad (72)$$

where

$$\kappa_n = \sqrt{(n\pi/2h)^2 + p^2}$$

Again, when the width of the plates is large compared to the separation such that  $|\pi/h| \gg |p|$  one can neglect the contribution from the sum in (72), in which case this equation can be written alternatively as

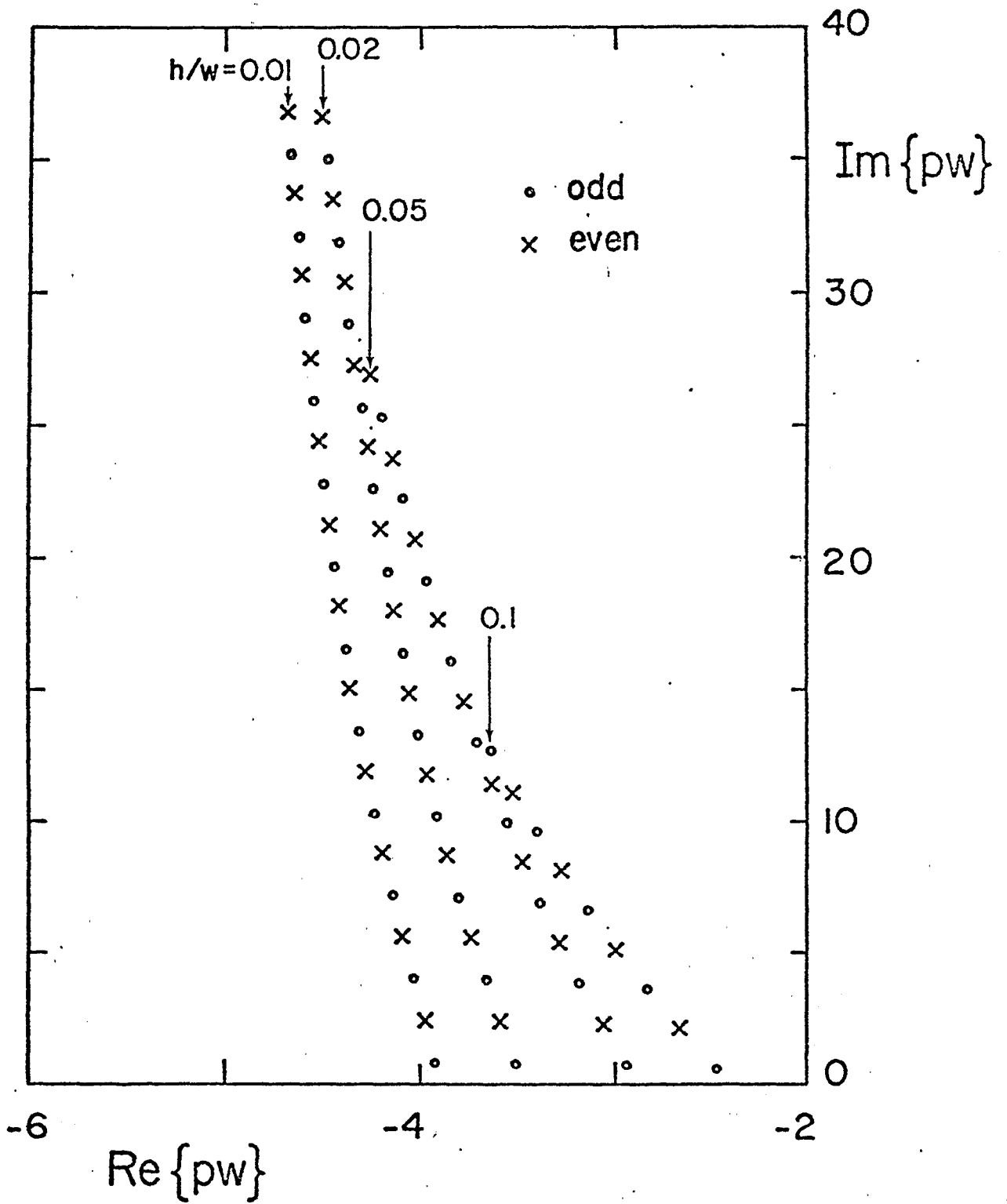


Figure 6. The roots of (70) and (71). Roots such that  $|ph| \ll 1$  are the transverse propagation constants for the anti-symmetric TM modes  $(p'_{a,n})$ .

$$\xi M(\xi) (2p + \xi)^{-1} e_s^e(\xi) + \int_0^\infty \frac{\exp(-2\xi'w) e_a^o(\xi')}{2p + \xi + \xi'} d\xi' = 0 \quad (73)$$

where

$$e_s^e(\xi) = \xi^{-1} k(\xi) \tilde{y}_a^o(p + \xi)$$

and  $k(\xi)$ ,  $M(\xi)$  are given by (55). For large values of  $|pw|$  the main contribution to the integral comes from small values of  $\xi'$ . By using small argument approximation of  $M(\xi)$  one gets

$$\pi\sqrt{\xi/2p} \exp(2pw) e_s^e(\xi) + \int_0^\infty \frac{\exp(-2\xi'w) e_a^o(\xi')}{2p + \xi + \xi'} d\xi' = 0 \quad (74)$$

and this equation shows that for small values of the argument one has

$$e_s^e(\xi) \approx e_s^e/\sqrt{\xi}. \quad (75)$$

Substituting this expression into (74) one obtains the following equation that  $p$  must satisfy in order for (74) to have a nontrivial solution

$$2\sqrt{\pi} \sqrt{pw} \exp(2pw) + 1 = 0 \quad (76)$$

For large values of  $|pw|$  this equation has the asymptotic solution

$$p_{s,n}^e w = (n + \frac{3}{8})\pi i - \frac{1}{4} \ln(4\pi^2 n) + O(n^{-1} \ln n) \quad (77)$$

whereas in the general case (76) was solved numerically and the results are presented in Fig. 5.

#### F. Odd, Symmetric TE Modes

Similarly, the transverse propagation constants for the odd, symmetric TE modes are determined from

$$2\sqrt{\pi} \sqrt{pw} \exp(2pw) + 1 = 0 \quad (78)$$

which for large values of  $|pw|$  has the asymptotic solution

$$p_{s,n}^{n0} w = \left(n - \frac{1}{8}\right) \pi i - \frac{1}{4} \ln(4\pi^2 n) + O(n^{-1} \ln n) \quad (79)$$

For not so large values of  $|pw|$  the solutions of (78) are presented in Fig. 5.

It is seen that the absolute value of the real part of the transverse propagation constant for the symmetric TE modes is smaller than that of the symmetric TM modes. This means of course that for high enough frequencies the TE modes are less attenuated than are the TM modes.

### G. Even, Antisymmetric TE Modes

It now remains to obtain the propagation constants for the antisymmetric TE modes. For large separation-to-width ratio the even, antisymmetric TE modes are determined by the nontrivial solutions of the integral equation

$$Q_+(q) \tilde{y}_a^e(q) + \frac{1}{2\pi i} \int_C \frac{\exp(-2q'w) \tilde{y}_a^e(q')}{(q'+q) Q_-(q')} dq' = 0 \quad (80)$$

Some care has to be exercised when evaluating the integral in (80) since  $Q_-(q)$  has a zero at  $q=p$ . In fact, by using the small argument expansion of  $Q_-(q)$  we obtain the following expression, valid in a neighborhood of  $q=p$ :

$$\frac{1}{Q_-(q)} \sim \frac{1}{Q_+(p)} \frac{1}{2ph(q-p)} \left[ 1 + ih \sqrt{2p(q-p)} \right], \quad q \sim p \quad (81)$$

By inserting the expression (81) for  $Q_-(q)$  into (80) and following a procedure similar to the one used previously in this section one obtains the following transcendental equation that  $p$  must satisfy

$$1 - \exp \left\{ 2pw + (2ph/\pi) [\ln(2\pi/ph) - \gamma + 1] \right\} - h \sqrt{p/w\pi} = 0 \quad (82)$$

where we have used the fact that

$$Q_+^2(p) \sim - (4hp^2) \exp \left\{ (2ph/\pi) [\ln(2\pi/ph) - \gamma + 1] \right\}$$

When  $h/w \ll 1$  then the solutions,  $p_{a,n}^{''e}$ , of (82) are given by

$$p_{a,n}^{''e} w = i\pi n \left\{ 1 - \frac{h}{w\pi} \left[ \ln \left( \frac{2\pi w}{nh} \right) - \gamma + 1 - \frac{1}{2\sqrt{2n}} \right] \right\} \\ - \frac{h}{w} \pi n \left[ \frac{1}{2} + \frac{1}{2\pi\sqrt{2n}} \right], \quad n = 1, 2, 3, \dots \quad (83)$$

In Fig. 7 the roots  $p_{a,n}^{''e}$  are displayed for some different values of  $h/w$ .

#### H. Odd, Antisymmetric TE Modes

In the same way, the transverse propagation constants  $p_{a,n}^{''o}$  of the odd, antisymmetric TE modes are given by the following expression

$$p_{a,n}^{''o} w = i\pi \left( n - \frac{1}{2} \right) \left\{ 1 - \frac{h}{w\pi} \left[ \ln \left( \frac{4\pi w}{(2n-1)h} \right) - \gamma + 1 - \frac{1}{2\sqrt{2n-1}} \right] \right\} \\ - \frac{h}{w} \pi \left( n - \frac{1}{2} \right) \left[ \frac{1}{2} + \frac{1}{2\pi\sqrt{2n-1}} \right], \quad h/w \ll 1. \quad (84)$$

and these values are graphed in Fig. 7.

Some comments are now in order concerning the results obtained for the transverse propagation constants. First of all, the antisymmetric TE modes have the smallest real part. This means of course that for high enough frequencies, the antisymmetric TE modes are the least attenuated ones. In the next section it will be seen that the antisymmetric TE modes are the modes with the highest field intensities between the plates. Therefore, besides the TEM mode, these modes are the most important ones inside a wide-plate simulator.

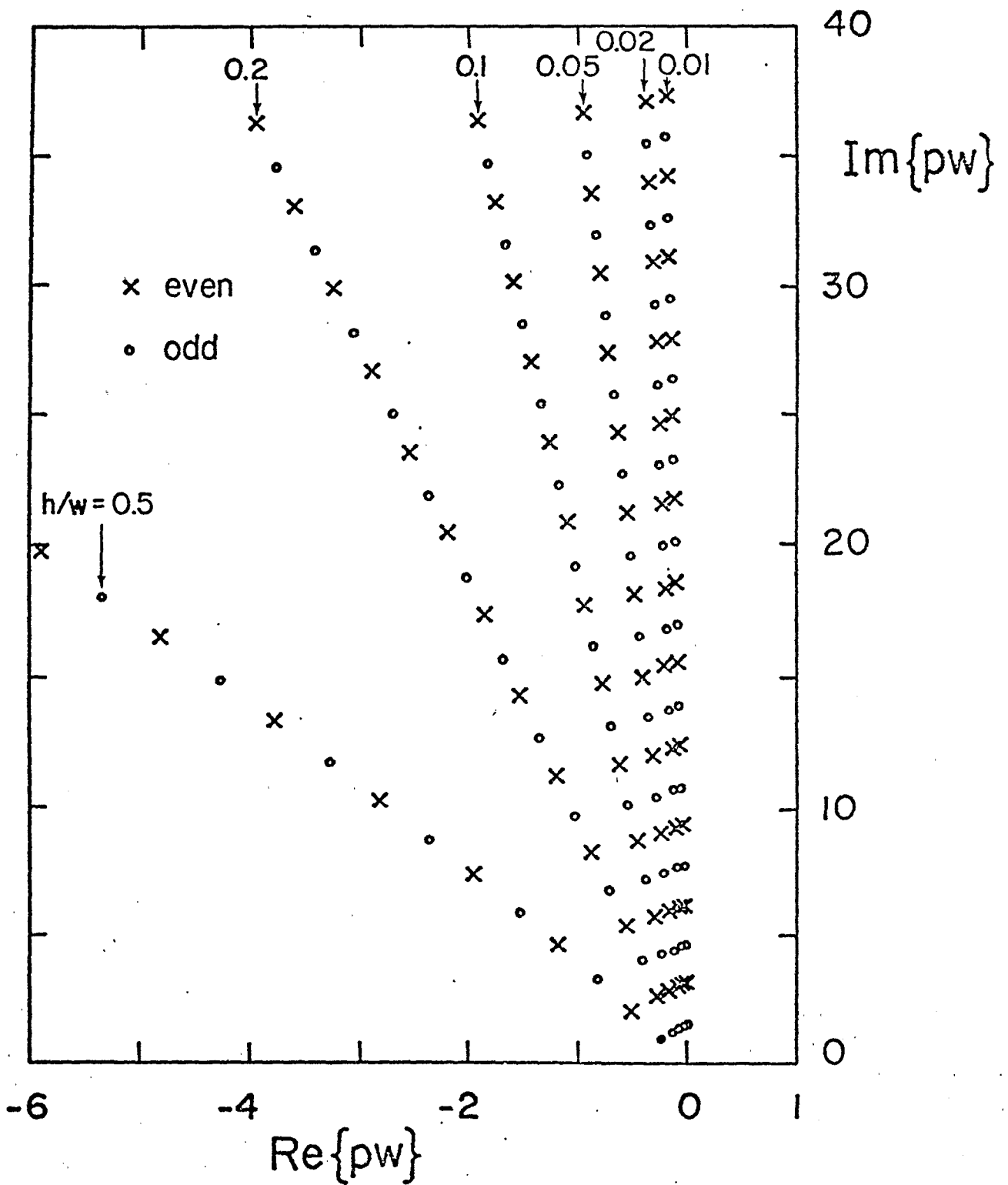


Figure 7. The transverse propagation constants for the antisymmetric TE modes  $(p_{a,n}^{\prime\prime})$ .

#### IV. FIELD DISTRIBUTION OF THE MODES

In this section, the field distribution of the different modes on the parallel-plate waveguide will be investigated. The main emphasis will be paid to the region between the plates, since this region is the region of interest for the simulator. The first part of this section deals with the TM modes and the second part with the TE modes.

##### A. Field Distribution of TM modes

As has been pointed out in the two previous sections the transverse magnetic modes can be classified as a combination of symmetric/antisymmetric and even/odd modes. The longitudinal component of the electric field of these modes are given by the following expressions, which are obtained from (4), (6), (17), (26), and (31),  $|y| < h$

$$\begin{aligned}
 E_{z,s}^e(x,y) &= \frac{1}{4\pi i} \int_C \tilde{x}_s^e(q) \exp(-qw) \cosh(qx) \frac{\sin[\kappa(y+h)] - \sin[\kappa(y-h)]}{\sin(2\kappa h)} dq \\
 E_{z,s}^o(x,y) &= \frac{1}{4\pi i} \int_C \tilde{x}_s^o(q) \exp(-qw) \sinh(qx) \frac{\sin[\kappa(y+h)] - \sin[\kappa(y-h)]}{\sin(2\kappa h)} dq \\
 E_{z,a}^e(x,y) &= \frac{1}{4\pi i} \int_C \tilde{x}_a^e(q) \exp(-qw) \cosh(qx) \frac{\sin[\kappa(y+h)] + \sin[\kappa(y-h)]}{\sin(2\kappa h)} dq \\
 E_{z,a}^o(x,y) &= \frac{1}{4\pi i} \int_C \tilde{x}_a^o(q) \exp(-qw) \sinh(qx) \frac{\sin[\kappa(y+h)] + \sin[\kappa(y-h)]}{\sin(2\kappa h)} dq.
 \end{aligned} \tag{85}$$

Since  $\tilde{x}_s^e$  is a holomorphic function to the right of  $C$  the integrals in (85) can be evaluated using residue calculus. When  $|x| < w$  one gets

$$\begin{aligned}
 E_{z,s}^e(x,y) &= \frac{1}{8h} \sum_{m=1}^{\infty} (-1)^m \frac{m\pi}{\kappa_m h} \tilde{x}_s^e(\kappa_m) \exp(-\kappa_m w) \cosh(\kappa_m x) \\
 &\quad \left[ \sin \frac{m\pi(y+h)}{2h} - \sin \frac{m\pi(y-h)}{2h} \right]
 \end{aligned} \tag{86}$$

and similarly for  $E_{z,s}^o$ ,  $E_{z,a}^o$ ,  $E_{z,a}^o$ . The quantity  $\kappa_m$  is given by

$$\kappa_m = \sqrt{\frac{m^2 \pi^2}{4h^2} + p^2} \approx \frac{m\pi}{2h} \quad (87)$$

since  $|ph| \ll 1$  for the modes of interest here. Therefore, each term in the sum (86) is very small provided that  $|w \pm x| > h$  and so the field of the TM modes is very weak between the two plates. Thus, the TM mode contribution to the electromagnetic field on a simulator consisting of two parallel, wide plates can be neglected. This is different from the narrow-plate case where besides the TEM mode the TM modes make up the major contribution to the electromagnetic field.

#### B. Field Distribution of TE modes

The field distribution of the TE modes are determined from the longitudinal component of the H-field,

$$\begin{aligned} H_{z,s}^e(x,y) &= \frac{1}{4\pi i} \int_C \tilde{y}_a^o(q) \exp(-qw) \sinh(qx) \frac{\cos[\kappa(y+h)] - \cos[\kappa(y-h)]}{\sin(2\kappa h)} dq \\ H_{z,s}^o(x,z) &= \frac{1}{4\pi i} \int_C \tilde{y}_a^e(q) \exp(-qw) \cosh(qx) \frac{\cos[\kappa(y+h)] - \cos[\kappa(y-h)]}{\sin(2\kappa h)} dq \\ H_{z,a}^e(x,z) &= \frac{1}{4\pi i} \int_C \tilde{y}_s^o(q) \exp(-qw) \sinh(qx) \frac{\cos[\kappa(y+h)] + \cos[\kappa(y-h)]}{\sin(2\kappa h)} dq \\ H_{z,a}^o(x,y) &= \frac{1}{4\pi i} \int_C \tilde{y}_s^e(q) \exp(-qw) \cosh(qx) \frac{\cos[\kappa(y+h)] + \cos[\kappa(y-h)]}{\sin(2\kappa h)} dq. \end{aligned} \quad (88)$$

These integrals can be evaluated with residue calculus thereby yielding

$$H_{z,a}^o(x,y) = \frac{1}{4ph} \tilde{y}_a^o(p) \exp(-pw) \cosh(px)$$

$$+ \frac{\pi}{8} \sum_{m=1}^{\infty} \frac{m(-1)^m}{\kappa_m^2 h^2} \tilde{y}_a^o(\kappa_m) \exp(-\kappa_m w) \cosh(\kappa_m x) \left[ \cos \frac{m\pi(y+h)}{2h} + \cos \frac{m\pi(y-h)}{2h} \right]$$

$$H_{z,a}^e(x,y) = \frac{1}{4ph} \tilde{y}_a^e(p) \exp(-pw) \sinh(px)$$

(89)

$$+ \frac{\pi}{8} \sum_{m=1}^{\infty} \frac{m(-1)^m}{\kappa_m^2 h^2} \tilde{y}_a^e(\kappa_m) \exp(-\kappa_m w) \sinh(\kappa_m x) \left[ \cos \frac{m\pi(y+h)}{2h} + \cos \frac{m\pi(y-h)}{2h} \right]$$

$$H_{z,s}^o(x,y) = \frac{\pi}{8} \sum_{m=1}^{\infty} \frac{m(-1)^m}{\kappa_m^2 h^2} \tilde{y}_s^o(\kappa_m) \exp(-\kappa_m w) \cosh(\kappa_m x) \left[ \cos \frac{m\pi(y+h)}{2h} - \cos \frac{m\pi(y-h)}{2h} \right]$$

$$H_{z,s}^e(x,y) = \frac{\pi}{8} \sum_{m=1}^{\infty} \frac{m(-1)^m}{\kappa_m^2 h^2} \tilde{y}_s^e(\kappa_m) \exp(-\kappa_m w) \sinh(\kappa_m x) \left[ \cos \frac{m\pi(y+h)}{2h} - \cos \frac{m\pi(y-h)}{2h} \right]$$

Since each term in the sums in (89) is very small when  $h \ll w$  and  $|wix| > h$  it is clear that only the antisymmetric TE modes constitute an important contribution to the simulator field. The only significantly contributing field components of the odd and even antisymmetric TE modes are, therefore, given by

$$H_{z,a}^o(x,y) \approx H_o \cosh(px)$$

$$H_{z,a}^e(x,y) \approx H_o \sinh(px)$$

$$E_{y,a}^o(x,y) \approx -(\mu_o s/p) H_o \sinh(px)$$

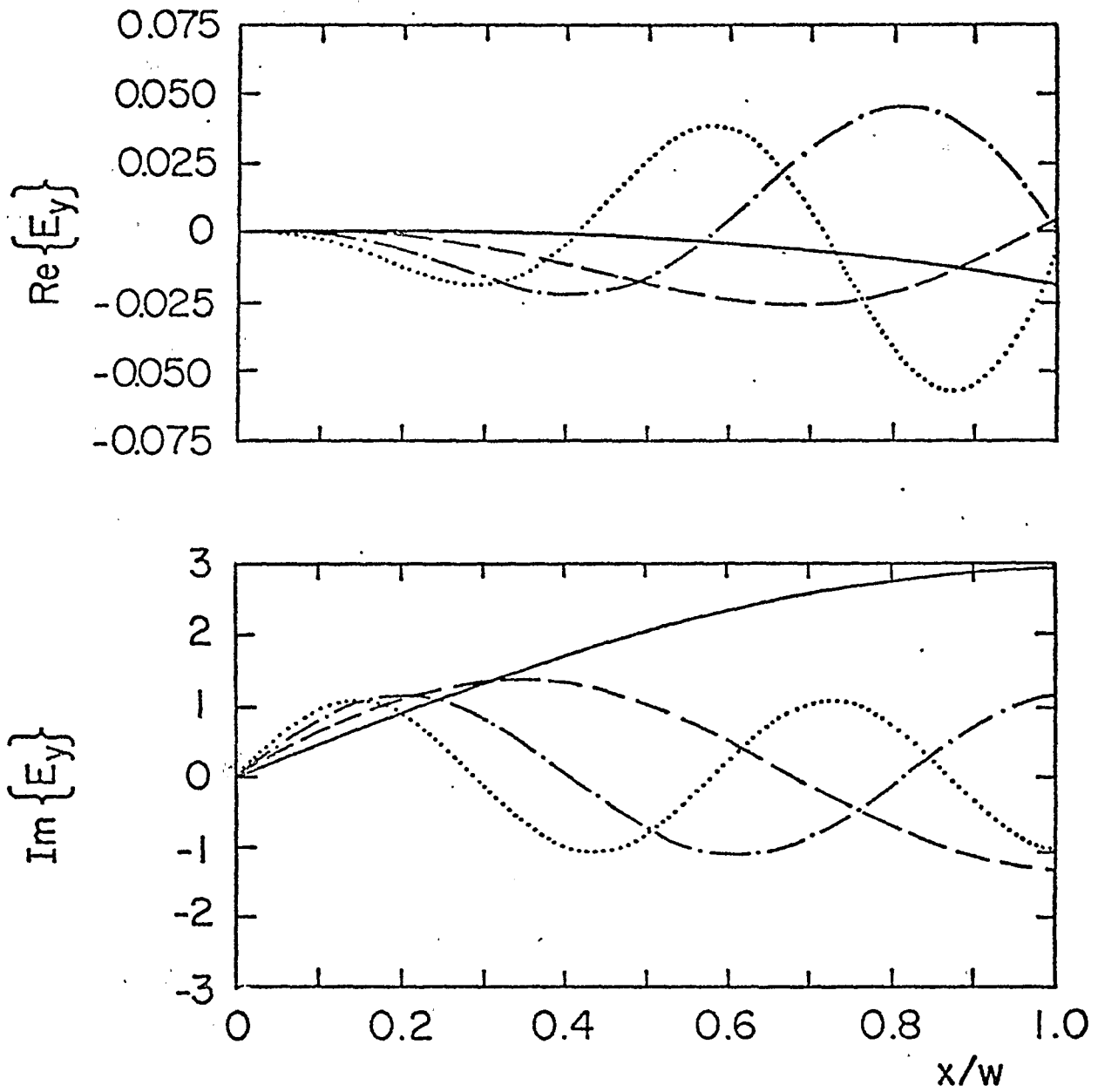
$$E_{y,a}^e(x,y) \approx -(\mu_o s/p) H_o \cosh(px) \quad (90)$$

$$H_{x,a}^o(x,y) \approx (\zeta/p) H_o \sinh(px)$$

$$H_{x,a}^e(x,y) \approx (\zeta/p) H_o \cosh(px)$$

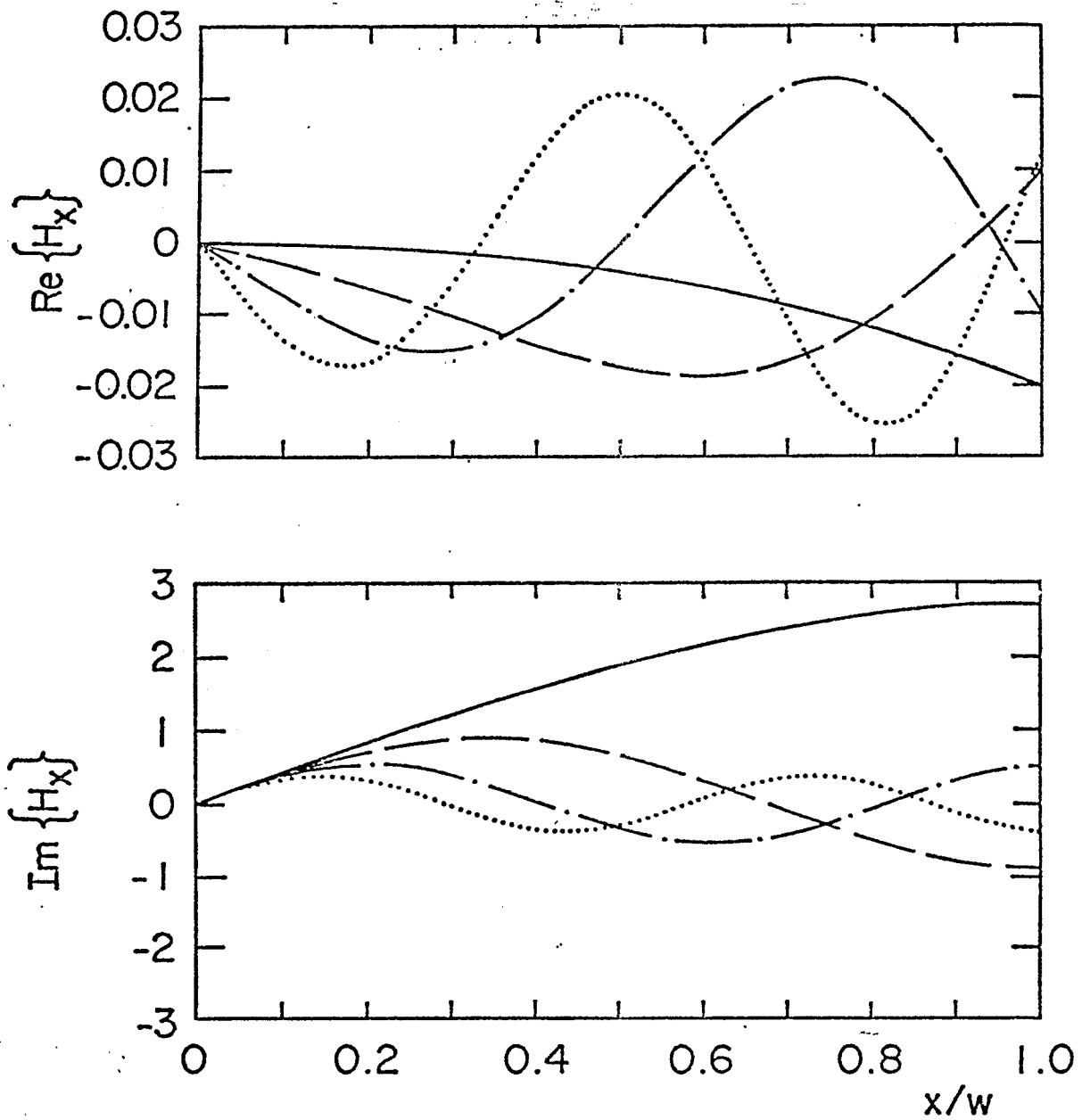
Graphs of the field distributions of the three lowest even and odd antisymmetric

TE modes are presented in Figs. 8 and 9. It is observed from these graphs that around the center of the simulator, the field of these modes can be expressed in terms of an almost real function. It is also noted that the magnitude of the field of these modes gets larger as the distance from the center of the waveguide increases.



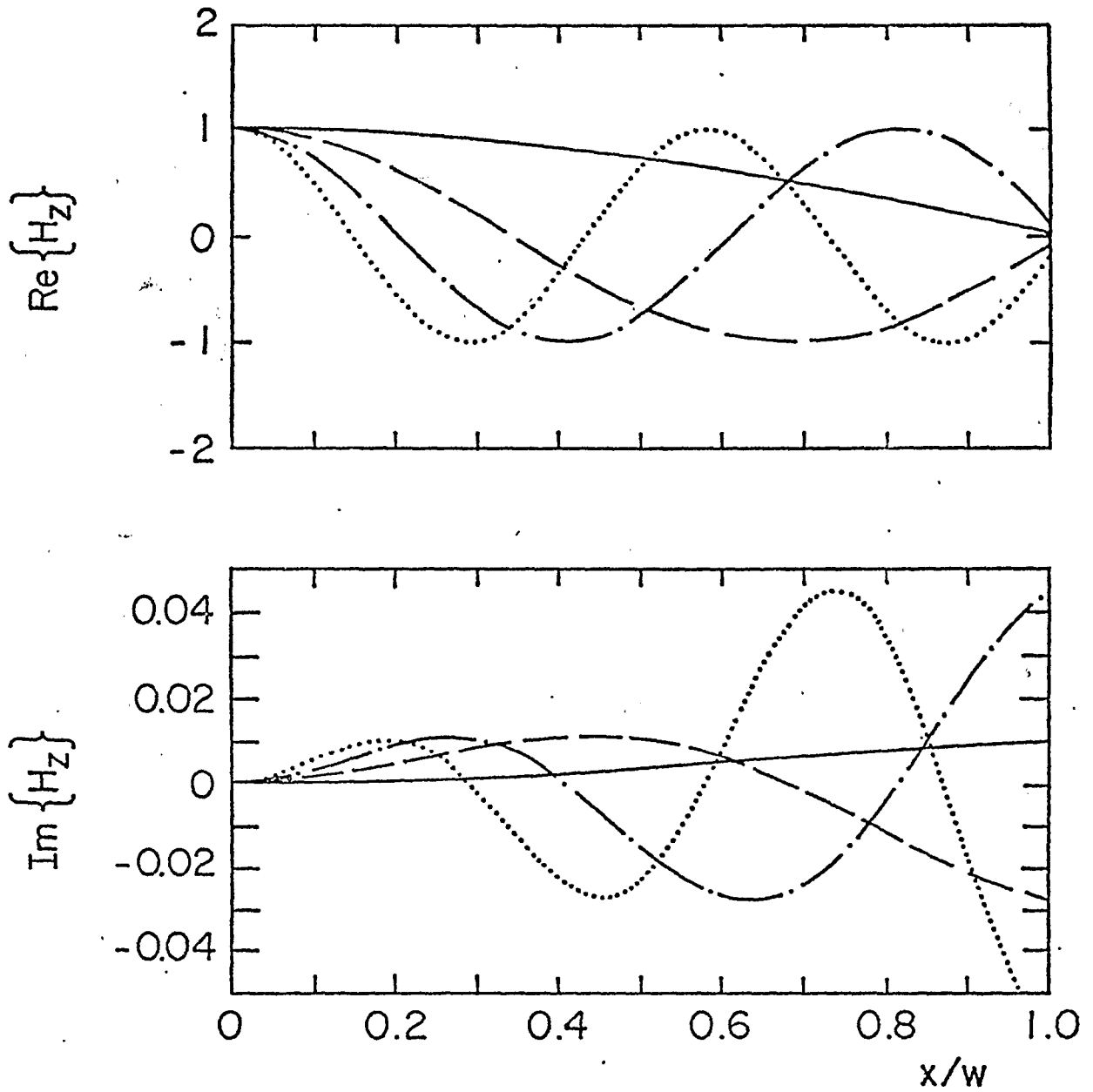
$\text{pw} = -0.010 - i1.54$  ———,  $-0.028 - i4.62$  — — —,   
 $-0.045 - i7.71$  - · - · - ·,  $-0.062 - i10.81$  ······.

Figure 8a. Transverse variation of the  $E_y$  field component of the four lowest odd antisymmetric TE modes.



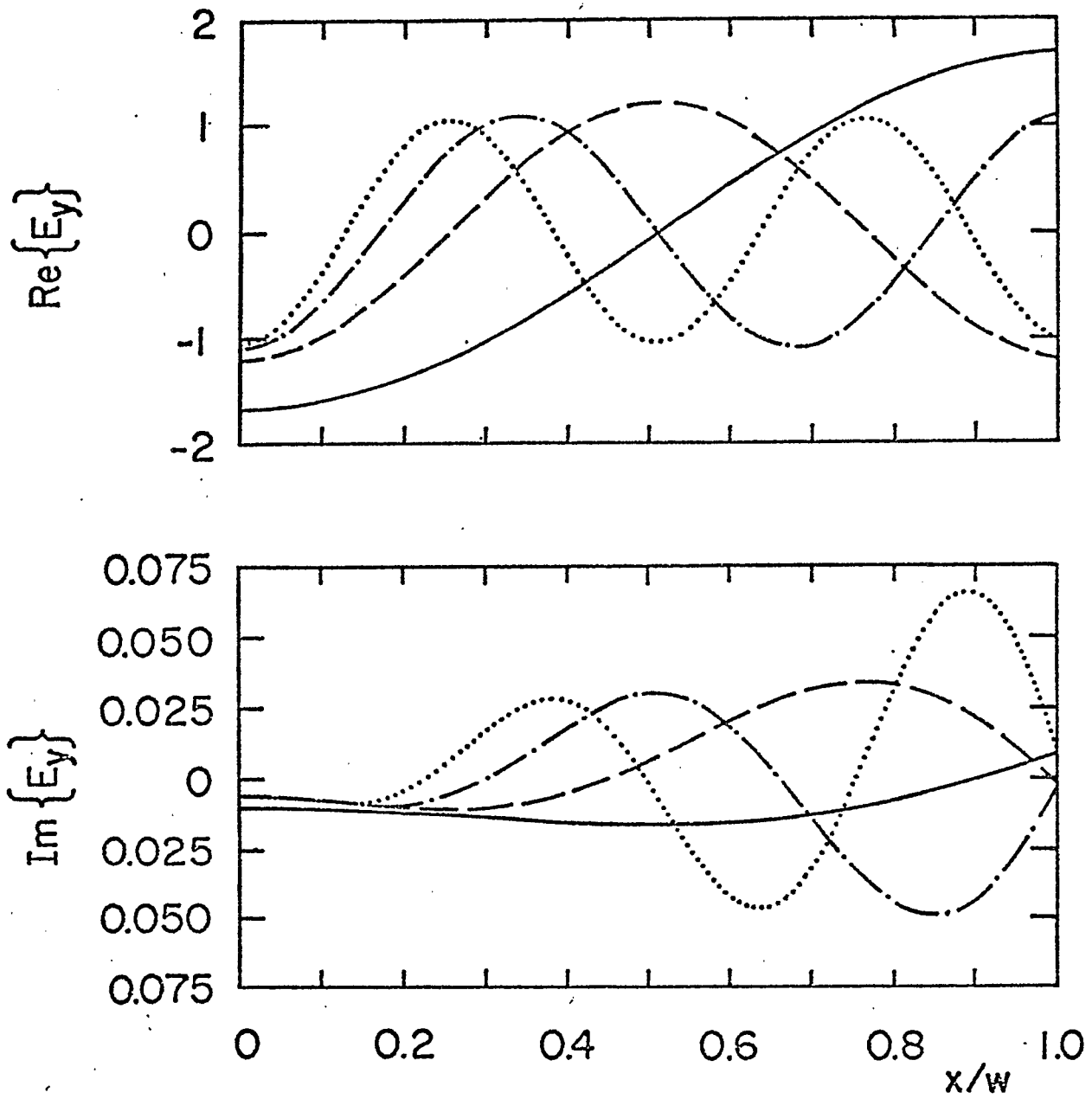
$\rho w = -0.010 - i1.54$  ———,  $-0.028 - i4.62$  — — —,   
 $-0.045 - i7.71$  - · - · - ·,  $-0.062 - i10.81$  ······.

Figure 8b. Transverse variation of the  $H_x$  field component of the four lowest odd antisymmetric TE modes.



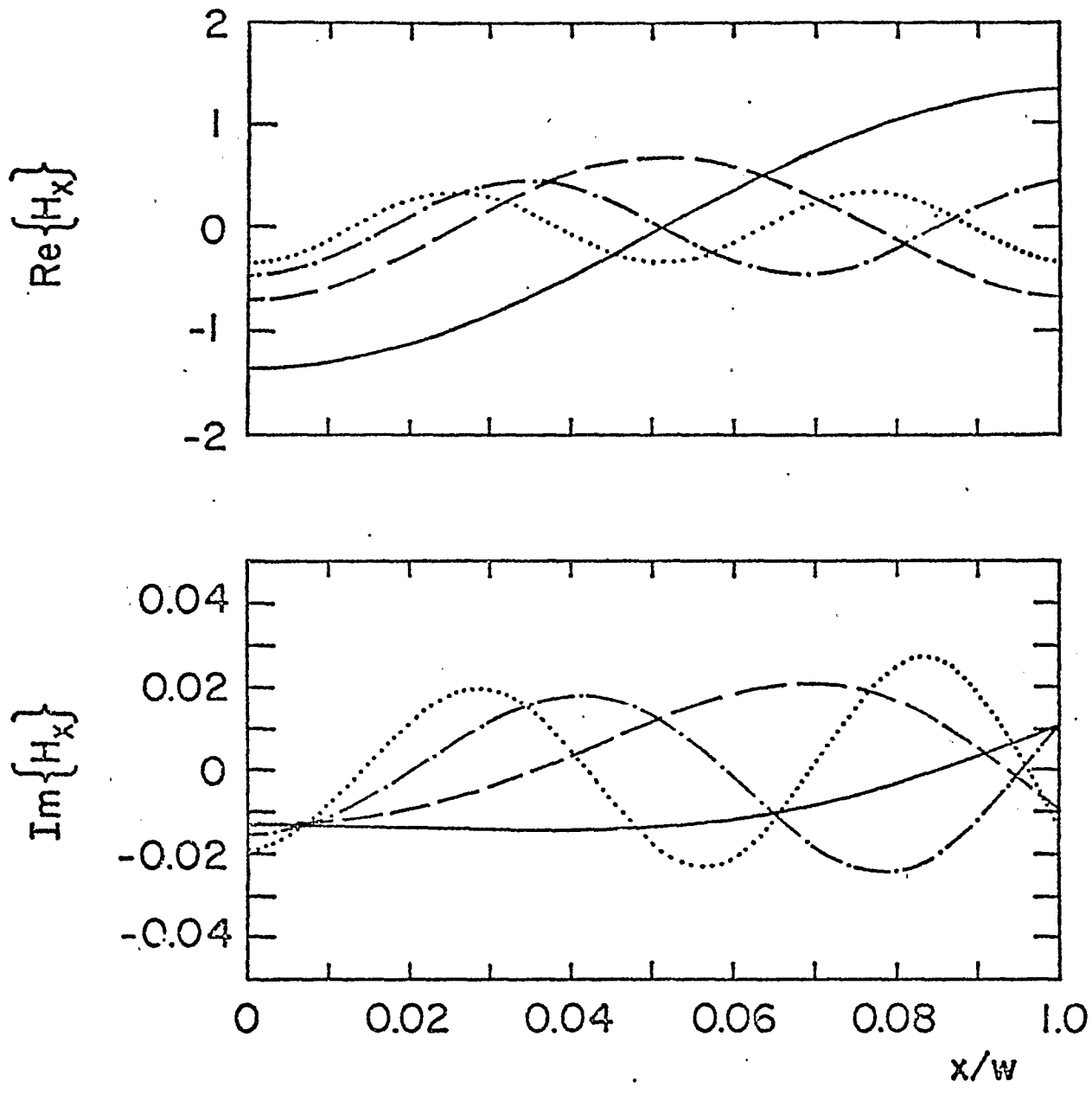
$\rho\omega = -0.010 - i1.54$  ———,  $-0.028 - i4.62$  ———,   
 $-0.045 - i7.71$  ———,  $-0.062 - i10.81$  .....

Figure 8c. Transverse variation of the  $H_z$  field component of the four lowest odd antisymmetric TE modes.



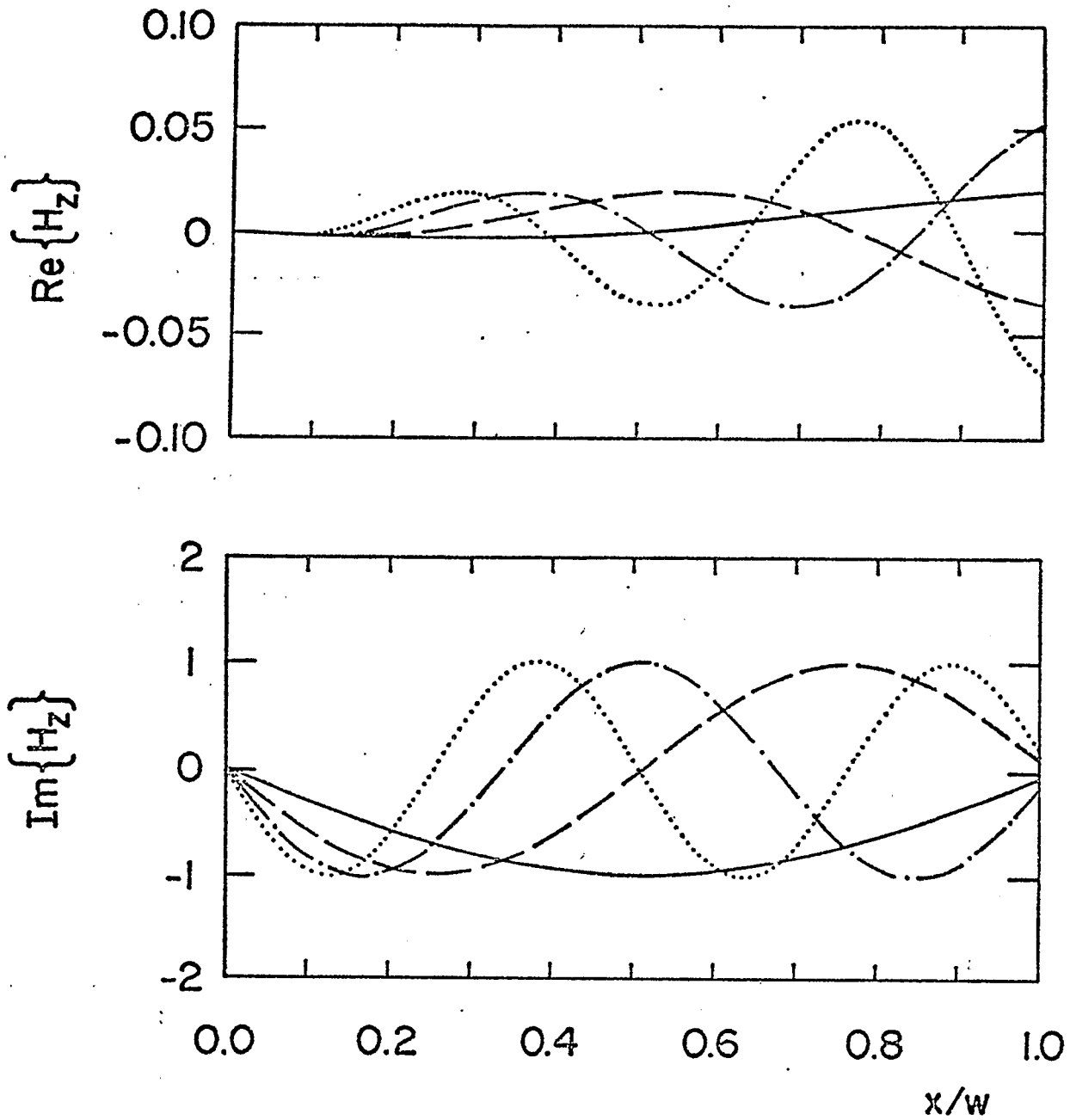
$\text{pw} = -0.019 - i3.08$  ———,  $-0.036 - i6.16$  ----,   
 $-0.053 - i9.26$  -·-·-·-,  $-0.070 - i12.35$  .....

Figure 9a. Transverse variation of the  $E_y$  field component of the four lowest even antisymmetric TE modes.



$p_w = -0.019 - i3.08$  ———,  $-0.036 - i6.16$  ----,  
 $-0.053 - i9.26$  -·-·-·-,  $-0.070 - i12.35$  .....

Figure 9b. Transverse variation of the  $H_x$  field component of the four lowest even antisymmetric TE modes.



$\text{pw} = -0.019 - i3.08$  ———,  $-0.036 - i6.16$  — — —,   
 $-0.053 - i9.26$  - · - · - ·,  $-0.070 - i12.35$  ······.

Figure 9c. Transverse variation of the  $H_z$  field component of the four lowest even antisymmetric TE modes.

## REFERENCES

1. C.E. Baum, "Impedances and Field Distributions for Parallel Plate Transmission Line Simulators," *Sensor and Simulation Note* 21, June 1966.
2. C.E. Baum, "General Principles for the Design of ATLAS I and II, Part V: Some Approximate Figures of Merit for Comparing the Waveforms Launched by Imperfect Pulser Arrays onto TEM Transmission Lines," *Sensor and Simulation Note* 148, May 1972.
3. A.E.H. Love, "Some Electrostatic Distributions in Two Dimensions," *Proc. London Math. Soc.*, Vol. 22, pp. 337 - 369, 1923.
4. T.L. Brown and K.D. Granzow, "A Parameter Study of Two-Parallel-Plate Transmission Line Simulators of EMP Sensor and Simulation Note 21," *Sensor and Simulation Note* 52, April 1968.
5. C.E. Baum, D.V. Giri, and R.D. Gonzalez, "Electromagnetic Field Distribution of the TEM Mode in a Symmetrical Two-Parallel-Plate Transmission Line," *Sensor and Simulation Note* 219, April 1976.
6. L. Marin, "Modes on a Finite-Width, Parallel-Plate Simulator. I. Narrow Plates," *Sensor and Simulation Note* 201, September 1974.
7. L. Marin, "Transient Electromagnetic Properties of Two Parallel Wires," *Sensor and Simulation Note* 173, March 1973.
8. D.S. Jones, "Diffraction by a Wave-Guide of Finite Length," *Proc. Camb. Phil. Soc.*, Vol. 48, pp. 118 - 134, 1952.
9. W.E. Williams, "Diffraction by Two Parallel Planes of Finite Length," *Proc. Camb. Phil. Soc.*, Vol. 50, pp. 309 - 318, 1954.
10. D.S. Jones, *The Theory of Electromagnetism*, Pergamon Press, London, 1964.
11. B. Noble, *Methods Based on the Wiener-Hopf Technique for the Solution of Partial Differential Equations*, Pergamon Press, London, 1958.
12. K. Westphal and H. Witte, "Zur Theorie einer Klasse von Beugungsproblemen mittels singulärer Integralgleichungen," part I, "'Klassische' Beugungsprobleme," *Ann. Phys.* Vol. 7, pp. 283 - 351, 1959, and part II, "Beugung skalarer hochfrequenter Wellen an einer Kreisblende," *Ann. Phys.* Vol. 20, pp. 14 - 28, 1967.
13. N.I. Muskhelishvili, *Singular Integral Equations*, Noordhoff, Groningen, 1953.
14. L.A. Weinstein, *Open Resonators and Open Waveguides*, The Golem Press, Boulder, 1969.
15. L.A. Weinstein, "Open Resonators for Lasers," *Sov. Phys. JETP*, Vol. 17, pp. 709 - 719, 1963.

16. T. Itoh and R. Mittra, "Resonance Conditions of Open Resonators at Microwave Frequencies," IEEE Trans. Microwave Theory and Techniques, Vol. MTT-22, February 1974.
17. E.N. Fox, "The Diffraction of Sound Pulses by an Infinitely Long Strip," Philos. Trans. Roy. Soc., A, Vol. 241, pp. 71-103, 1948.
18. R.F. Millar, "Diffraction by a Wide Slit and Complementary Strip, I," Proc. Camb. Phil. Soc., Vol. 54, pp. 479-496, 1958.
19. R.F. Millar, "Diffraction by a Wide Slit and Complementary Strip, II," Proc. Camb. Phil. Soc., Vol. 54, pp. 497-511, 1958.
20. G.A. Grinberg, "A New Method for Solving Problems Related to the Diffraction of Electromagnetic Waves by a Plane with an Unbounded Straight Slit," Sov. Phys. Techn. Phys., Vol. 27, pp. 2410-2419, 1957.
21. G.A. Grinberg, "A Method for Solving Problems of the Diffraction of Electromagnetic Waves by Ideally Conducting Plane Screens, Based on the Study of the Currents Induced on the Shaded Side of the Screen," part I, "General Foundations of the Method," Sov. Phys. Techn. Phys., Vol. 3, pp. 509-520, 1958 and part II, "Diffraction by a Half-Plane and a Plane with an Infinitely Long Straight Slit," Sov. Phys. Techn. Phys., Vol. 3, pp. 521-533, 1958.
22. M.D. Khaskind and L.A. Weinstein, "Diffraction of Plane Waves by a Slit and a Tape," Radio Eng. Electronic Phys., Vol. 10, pp. 1492-1501, 1964.
23. T.T. Wu, "Theory of Microstrips," J. Appl. Phys., Vol. 28, pp. 299-302, 1957.
24. T. Itoh and R. Mittra, "Analysis of Modes in a Finite-Width Parallel-Plate Waveguide," Sensor and Simulation Note 208, January 1975.